JACS
JOURNAL OF THE AMERICAN CHEMICAL SOCIETY
pubs.acs.org/JACS
Article

Marriage of Peroxides and Nitrogen Heterocycles: Selective Three-Component Assembly, Peroxide-Preserving Rearrangement, and Stereoelectronic Source of Unusual Stability of Bridged Azaozonides

Ivan A. Yaremenko,* Yulia Yu. Belyakova, Peter S. Radulov, Roman A. Novikov, Michael G. Medvedev, Nikolai V. Krivoshchapov, Alexander A. Korlyukov, Igor V. Alabugin,* and Alexander O. Terent'ev*

Cite This: J. Am. Chem. Soc. 2021, 143, 6634–6648

ABSTRACT: Stable bridged azaozonides can be selectively assembled via a catalyst-free three-component condensation of 1,5-diketones, hydrogen peroxide, and an NH-group source such as aqueous ammonia or ammonium salts. This procedure is scalable and can produce gram quantities of bicyclic stereochemically rich heterocycles. The new azaozonides are thermally stable and can be stored at room temperature for several months without decomposition and for at least 1 year at −10 °C. The chemical stability of azaozonides was explored for their subsequent selective transformations including the first example of an aminoperoxide rearrangement that preserves the peroxide group. The amino group in aminoperoxides has remarkably low nucleophilicity and does not participate in the usual amine alkylation and acylation reactions. These observations and the 15 pK_a units decrease in basicity in comparison with a typical dialkyl amine are attributed to the strong hyperconjugative $n_N \rightarrow \sigma^*_{C-O}$ interaction with the two antiperiplanar C−O bonds. Due to the weakness of the complementary $n_O \rightarrow \sigma^*_{C-N}$ donation from the peroxide oxygens (a consequence of "inverse α-effect"), this interaction depletes electron density from the NH moiety, protects it from oxidation, and makes it similar in properties to an amide.

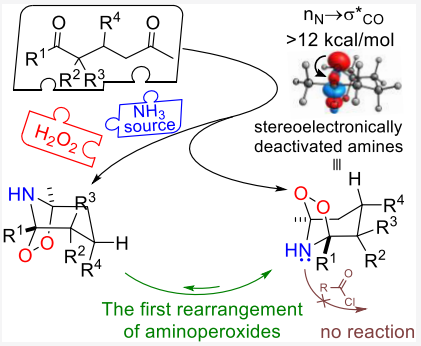

INTRODUCTION

Organic peroxides offer a largely uncharted chemical space for the development of new medicinal agents with antimalarial,[1−9] anthelmintic,[10−15] anticancer,[16−26] fungicidal,[26,27] antitubercular,[28−30] and antiviral[31−33] activities. Artemisinin, a natural peroxide recognized by the 2015 Nobel Prize in Medicine to Youyou Tu, and its synthetic analogues such as arterolane are important antimalarial drugs. Furthermore, both artemisinin and the ethanolic extract of *Artemisia annua* L. are highly potent at inhibiting the proliferating ability of SARS-CoV-2 (the COVID-19-causing virus).[34−36]

The dramatic expansion of medicinal chemistry of organic peroxides was inspired by >100 known peroxide-containing natural products.[37−39] The variety of natural examples lessened concerns associated with the perceived peroxide instability and led to research efforts aimed at the development of synthetic approaches to varied classes of cyclic peroxides including 1,2-dioxolanes,[40−50] 1,2,4-trioxolanes (ozonides),[26,51−58] 1,2-dioxanes,[59−64] 1,2,4-trioxanes,[65−69] 1,2,4,5-tetraoxanes,[70−72] cyclic triperoxides,[73] and tricyclic mono- and bisperoxides.[74−76]

However, notwithstanding the significant advances in the medical chemistry of peroxides, azaperoxides remain mostly unexplored. Only two natural azaperoxides, verruculogen[77−81] and fumitremorgin A,[82,83] are known (isolated from *Aspergillus fumigatus* in the 1970s, Figure 1). The challenging nature of these molecules is illustrated by the fact that their first total synthesis was developed only in 2015 by Baran's group.[84]

The few known "unnatural" amino peroxides reveal promising biological activity. For example, 11-aza-artemisinin, i.e., the product of replacement of the ester moiety of artemisinin with an amide group, is more potent against malaria than artemisinin itself.[85−87] Furthermore, both 11-aza-artemisinin and 6-aza-artemisinin exhibit anticancer activity.[88−90]

Hence, the development of stable and easily accessible cyclic peroxides fused to a nitrogen heterocycle remains an important problem. Although the introduction of a nitrogen atoms can dramatically expand the choices of possible peroxide-containing functionalities and strongly affect their interaction with biological targets, the lack of available synthetic approaches and intrinsic instability left azaperoxides in the shadow of artemisinin and other classic peroxides.

Received: February 27, 2021
Published: April 20, 2021

https://doi.org/10.1021/jacs.1c02249
J. Am. Chem. Soc. 2021, 143, 6634−6648

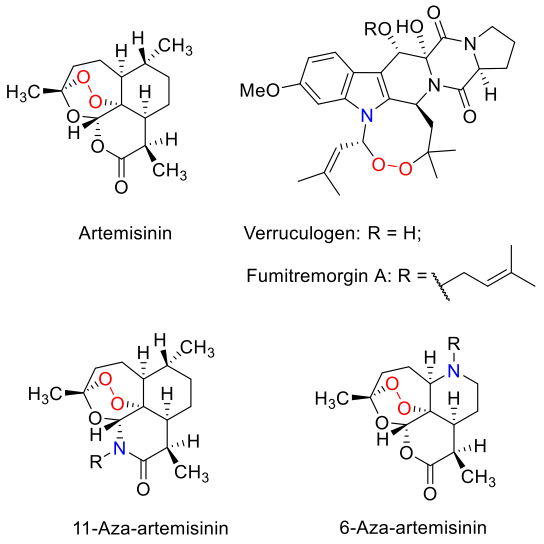

Figure 1. Structures of artemisinin and bioactive azaperoxides.

The main expected reason for the instability of azaperoxides is their self-oxidation due to the presence of both an oxidizing and a reducing part in the molecule. Oxidation of amines with hydrogen peroxide is well known and used for the synthesis of nitroso and nitro derivatives,[91,92] nitrones/*N*-oxides,[93−95] and imines.[96,97]

The instability of aminoperoxides and the difficulty of their isolation and purification impose significant limitations on the development of methods for their synthesis. The first attempts to synthesize azaperoxides from highly reactive acyclic monoketones, aldehydes, and small ring size cyclic ketones were reported by E. G. E. Hawkins[98−100] in the 1970s. The yields of aminoperoxides did not exceed 40%. In addition, attempts have been made to synthesize azaperoxides by other methods, such as ozonolysis of vinyl ether in the presence of imines,[101] ozonolysis of alkenes in the presence of primary amines,[102] and ozonolysis of the *O*-methylated dioximes.[103−105] In all cases, 1,2,4-dioxazolidines were obtained, at best, in moderate yields, and ozone, a toxic gas that has to be generated on demand, was required. 1,2,4-Dioxazolidines can also be prepared by oxidation of aziridines with singlet oxygen, but in a low yield.[106−108] One should also note the more recent approaches to the synthesis of 8- and 11-membered cyclic aminoperoxides via opening/recyclization of pentaoxaspiroalkanes with arylamines,[109] condensation of pentane-1,5-dial with *gem*-bis-hydroperoxides and primary amines,[110] and interaction of heptaoxaspiroalkanes with diamines.[110] However, the need to start with the less accessible cyclic bis- or trisperoxides significantly limits the scope of the products.

Selective synthesis of azaperoxides from diketones remains a challenge. For example, literature reports indicate that synthesis of cyclic aminoperoxide from a diketone (hexane-2,5-dione) was not possible due to steric reasons.[99] Also, the condensation of diketones with hydrogen peroxide and ammonia can lead to the formation of a complex mixture of products, both peroxide and non-peroxide in nature.

Furthermore, even though little is known about the chemistry of aminoperoxides, there are indications that they are capable of useful transformations. For example, it was found that substituted 1,2,4-dioxazolidines are convenient starting substrates for the synthesis of caprolactam and 11-cyanoundecanoic acid as a precursor for polymer Nylon-12.[111]

In this study, we resurrect peroxidative three-component co-condensations of ketones as a preparative approach to peroxy N-heterocycles and describe a convenient approach to the selective assembling of stable bridged azaozonides via a condensation of 1,5-diketones with hydrogen peroxide and an NH-group source. We also report that the new azaperoxides are sufficiently stable to participate in a variety of further chemical transformations including the first example of an azaperoxide rearrangement that preserves the peroxide group.

RESULTS AND DISCUSSION

Three-Component Condensation of 1,5-Diketones with Hydrogen Peroxide and NH-Group Source with the Formation of Bridged 1,2,4-Dioxazolidines (Bridged Azaozonides). The catalyst-free three-component condensation of 1,5-diketones **1a−u** with hydrogen peroxide and an NH-group source can be accomplished with aqueous H_2O_2 and a variety of NH-group sources such as aqueous NH_3, ammonium acetate, ammonium formate, and ammonium carbonate. In all cases bridged 1,2,4-dioxazolidines (bridged azaozonides) **2a−u** and **3a−r** are formed (Scheme 1 and Scheme 2). Unlike two-component condensation of 1,5-diketones with hydrogen peroxide, Lewis acid catalysis is not necessary.

Condensation of ethyl 2-acetyl-2-(4-chlorobenzyl)-5-oxohexanoate (**1l**) with a nitrogen source and hydrogen peroxide was used to study the effect of the nature and amount of the N-component, hydrogen peroxide, solvent, and reaction time on the yield of stereoisomeric bridged azaozonides **2l** and **3l** (Table 1; for additional experiments see Table S1 in the Supporting Information). A preliminary procedure for condensation of diketone **1l** with H_2O_2 and an NH-group source was as follows: an NH_3 source and aqueous H_2O_2 were added to a solution of the diketone **1l** (0.300 g; 0.92 mmol) in a solvent at room temperature. After completion, the solvent, an excess of ammonia, and hydrogen peroxide were removed in a vacuum of a membrane pump at 40−50 °C.

Condensation of 1,5-diketone **1l** with 34% aqueous H_2O_2 and 22% aqueous NH_3 in MeOH at a molar ratio 1,5-diketone **1l**:H_2O_2:NH_3 = 1:1.5:10 led to the formation of bridged azaozonides in 84% yield with the ratio **2l**:**3l** = 71:29 after 5 h (run 1, Table 1). The yield of **2l** + **3l** and molar ratio **2l**:**3l** were determined from the ^{1}H NMR data. In DMF and THF, the azaozonides **2l** + **3l** were obtained in 54% and 60% yields, respectively, in ∼40:60 **2l**:**3l** ratios (runs 2 and 3, Table 1). With acetonitrile (run 4), azaozonides were not observed. Under these conditions, acetonitrile was converted to acetamide faster than the aminoperoxide was formed. The optimal molar ratio for the condensation of 1,5-diketone **1l** with H_2O_2 and NH_3 was found to be **1l**:H_2O_2:NH_3 = 1:1.5:5, and the reaction was complete in 1.5 h (run 5; for additional experiments see Table S1 in the Supporting Information (SI)).

After finding the optimal conditions, we used ^{1}H NMR to monitor the formation of azaozonides **2l** and **3l** from 1,5-diketone **1l**, H_2O_2(aq), and NH_3(aq) in CD_3OD at 25 °C for 36 h (^{1}H NMR monitoring is presented in the SI). We found that azaozonide **3l** is a product of kinetic control, and azaozonide **2l** is a product of thermodynamic control. Also, ^{1}H NMR monitoring demonstrated that 1.5 h after the start of the reaction, the **2l**:**3l** ratio was 37:63 (see the SI). However, the **2l**:**3l** ratio changed to 87:13 after the reaction workup that included removal of the solvent, excess of ammonia, and H_2O_2 (run 5 of Table 1). Taking into account these results, we

https://doi.org/10.1021/jacs.1c02249
J. Am. Chem. Soc. 2021, 143, 6634−6648

Scheme 1. Structures and Isolated Yields of the Isomeric Mixtures of Azaozonides 2a−r and 3a−r, Synthesized from 1,5-Diketones 1a−r[a]

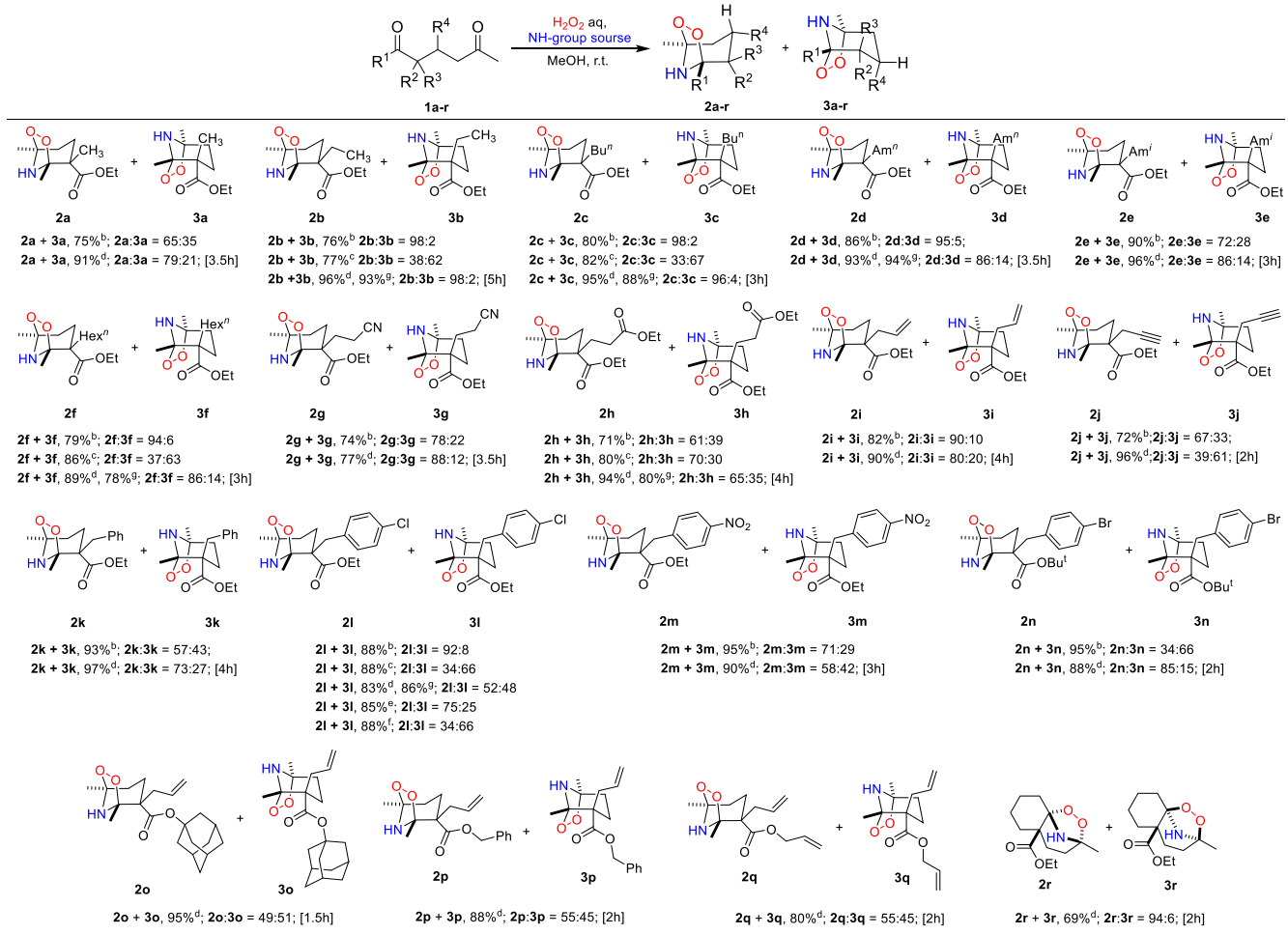

[a]In brackets the time of the reaction. The ratio of **2a−r**:**3a−r** is the average of three experiments. [b]Under conditions of run 5, Table 1. [c]Under conditions of run 6, Table 1. [d]Under conditions of run 7, Table 1. [e]Under conditions of run 8, Table 1. [f]Under conditions of run 9, Table 1. [g]Scaled to 1.0 g of 1,5-diketone **1** in the conditions of run 7, Table 1.

decided to change the procedure for the isolation of azaperoxides from the reaction mixture. The extraction of azaozonides directly from the reaction mixture with $CHCl_3$ allowed us to obtain the target azaozonides **2l** + **3l** in a 94% yield and 33:67 ratio (run 6, Table 1).

However, isolation of the individual azaozonides from the reaction mixture was not entirely trivial. The usual SiO_2 column chromatography with PE/EA as an eluent (run 5) provided azaozonides **2l** + **3l** in only 66% yields with the ratio **2l**:**3l** = 95:5. The 30% loss in the isolated yield in comparison with the NMR yield suggested that azaozonide **3l** may be more sensitive to the acidic nature of SiO_2 and degrades preferentially relative to azaozonide **2l** during column chromatography (see the Computational Analysis section for additional details). However, using 1 vol % Et_3N in $CHCl_3$ as eluent allowed us to isolate **2l** + **3l** in 83−88% yields without significant changes in the ratio **2l**:**3l** in comparison with the ^1H NMR of the reaction mixtures (runs 5−9).

Surprisingly, not only NH_3(aq), but also the ammonium salts, such as ammonium acetate, ammonium formate, and ammonium carbonate, can be used as an NH-group source in the three-component condensation of 1,5-diketone **1l**. To our knowledge, there are no literature examples of the synthesis of azaperoxides from ammonium salts. These salts are more convenient for dosing and using than NH_3(aq). By using NH_4OAc and $(NH_4)_2CO_3$, azaozonides **2l** + **3l** were obtained in 83% and 88% isolated yields, respectively (runs 7 and 9, Table 1). With $(NH_4)_2CO_3$, the full conversion of diketone **1l** was achieved in 3 h, rather than 1.5 h for NH_4OAc. In the case of ammonium formate, azaozonides **2l** + **3l** were obtained in 85% isolated yield in a ratio **2l**:**3l** = 75:25 (run 8). With $(NH_4)_2SO_4$, the target azaozonides were obtained only in trace amounts. The conditions of entry 7 of Table 1 were chosen as optimal when using ammonium salts as the NH source.

In the next step, we applied the optimized conditions to explore the scope and limitations of the assembly of azaozonides by introducing substituents R^1−R^4 at different positions in the 1,5-dicarbonyl compound **1**. Azaozonides **2a−r** and **3a−r** with various substituents were synthesized from 1,5-diketones **1a−r** (Scheme 1). The NH_4OAc-promoted reaction was monitored by TLC until complete conversion of the starting 1,5-diketones **1a−r**. Under conditions 7 of Table1, the three-component condensations of 1.0 g of 1,5-diketone **1** formed azaperoxides **2b** + **3b**, **2c** + **3c**, **2d** + **3d**, **2f** + **3f**, **2h** + **3h**, and **2l** + **3l** in isolated yields of 93%, 88%, 94%, 78%, 80%, and 86%, respectively. Although the diastereoisomeric bridged

https://doi.org/10.1021/jacs.1c02249
J. Am. Chem. Soc. 2021, 143, 6634−6648

Table 1. Synthesis of Stereoisomeric Bridged Azaozonides 2l and 3l via Condensation of 1,5-Diketone 1l with H_2O_2 and an NH-Group Source[a]

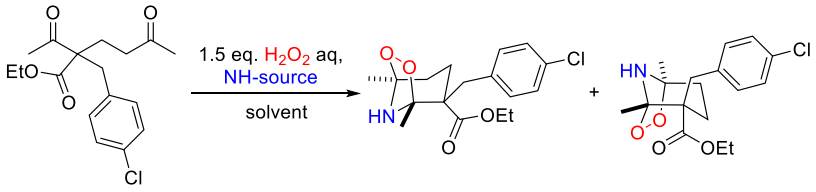

1l 2l 3l

run	NH-group source (equiv vs 1l)	solvent	time, h	NMR yield of 2l + 3l, % (isolated yield)	ratio of 2l:3l
1	NH_3 aq (10)	MeOH	5	84	71:29
2	NH_3 aq (10)	DMF	5	54	39:61
3	NH_3 aq (10)	THF	5	60	37:63
4	NH_3 aq (10)	CH_3CN	5		
5	NH_3 aq (5)	MeOH	1.5	94	87:13
				(66)[d]	95:5
				(88)[e]	92:8
6[b]	NH_3 aq (5)	MeOH	1.5	94	33:67
				(88)[e]	34:66
7[c]	NH_4OAc (5)	MeOH	1.5	95	52:48
				(83)[e]	52:48
8[c]	$HCOONH_4$ (5)	MeOH	1.5	94	75:25
				(85)[e]	75:25
9[c]	$(NH_4)_2CO_3$ (5)	MeOH	3	95	36:64
				(88)[e]	34:66

[a]22% NH_3(aq) (0.39−0.77 mL, 4.60−9.20 mmol, 5−10 mol of NH_3/1 mol of **1l**), NH_4OAc (0.355 g; 4.60 mmol), $HCOONH_4$ (0.290 g; 4.60 mmol) or $(NH_4)_2CO_3$ (0.442 g; 4.60 mmol), and 34% H_2O_2(aq) (0.12 mL, 1.38 mmol; 1.5 mol of H_2O_2/1 mol of **1l**) were successively added with stirring to a solution of 1,5-diketone **1l** (0.300 g; 0.92 mmol) in MeOH, DMF, THF or CH_3CN (10 mL) at 20−25 °C. In the case of $(NH_4)_2CO_3$, an additional 1 mL of H_2O was added to the reaction mixture. The reaction mixture was stirred at 20−25 °C for 1.5−5 h. The solvent, excess of ammonia, and H_2O_2 were removed in a vacuum of a membrane pump at 40−50 °C. The yields of **2l** and **3l** were determined from the ^{1}H NMR spectroscopic data. Molar ratio **2l**:**3l** is a mean from three experiments. [b]The procedure for the isolation of azaozonides **2l** + **3l** from the reaction mixture: $CHCl_3$ (30 mL) and water (10 mL) were added to the reaction mixture. The organic phase was separated; the aqueous phase was washed by $CHCl_3$ (3 × 30 mL). The combined organic phases were dried over $MgSO_4$ and filtered. The solvent was removed in the vacuum of a membrane pump at 20−25 °C. The yield of **2l** and **3l** was determined from the ^{1}H NMR spectroscopic data. [c]The procedure for the isolation of azaozonides **2l** + **3l** from the reaction mixture: $CHCl_3$ (30 mL) and NaOH (5% aqueous solution, 10 mL) were added to the reaction mixture. For the next steps see footnote *b*. [d]The mixture of azaozonides **2l** and **3l** was isolated by chromatography on SiO_2 using PE:EA = 20:1. [e]The mixture of azaozonides **2l** and **3l** was isolated by chromatography on SiO_2 using 1% Et_3N in $CHCl_3$.

azaozonides **2a−r** and **3a−r** could not be separated using conditions that worked for structurally similar diastereoisomeric bridged ozonides,[21,26,56] we were able to separate azaozonides **2m** + **3m** by ordinary column chromatography. The structure and stereochemistry of peroxides **2m** and **3m** were unambiguously established by X-ray crystallography. Both azaozonides are crystalline compounds that melt without decomposition at 136−138 °C and 120−122 °C, respectively. An interesting result was obtained with the aminoperoxidation of diketones **1s−v** that have a single substituent at the tether connecting the two ketone groups (Scheme 2). Under the conditions of entry 7, Table 1, the reaction was carried out until complete conversion of the starting 1,5-diketones **1s−v**. In the case of diketone **1v**, we obtained a complex mixture of products. The presence of the ester group in the α position of the diketone **1v** promotes its enolization, which probably contributes to the formation of the dihydropyridine ring rather than an aminoperoxide. According to NMR data, dihydropyridine **A** and pyridine **B** were in the mixture, while the target azaperoxide **2u** was absent. However, azaozonides **2s−u** were obtained in 37−78% isolated yields from diketones **1s−u** (Scheme 2). The structure of **2t** was unambiguously established by X-ray crystallographic analysis.

Scheme 2. Attempted Peroxidative Condensations of 1,5-Diketones 1s−v in the Presence of NH_4OAc

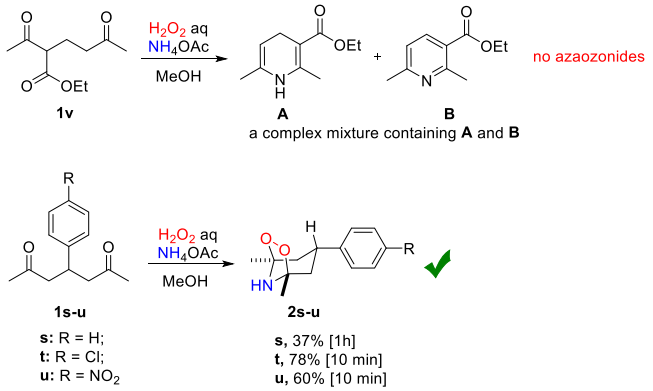

Stereochemical analysis of azaozonides **2a−r** and **3a−r** was performed based on the ^{15}N and key ^{1}H chemical shifts in combination with NOE data. For 2-CO_2R-substituted azaozonides **2a−r** and **3a−r**, both diastereomers have characteristic ^{15}N chemical shifts (Figure 2, A) that makes them easy to distinguish by conventional ^{1}H−^{15}N HSQC experiments. Also, the stereoisomer **3** has a characteristic signal of one proton of the CH_2 group in the ^{1}H NMR spectra; its

https://doi.org/10.1021/jacs.1c02249
J. Am. Chem. Soc. 2021, 143, 6634−6648

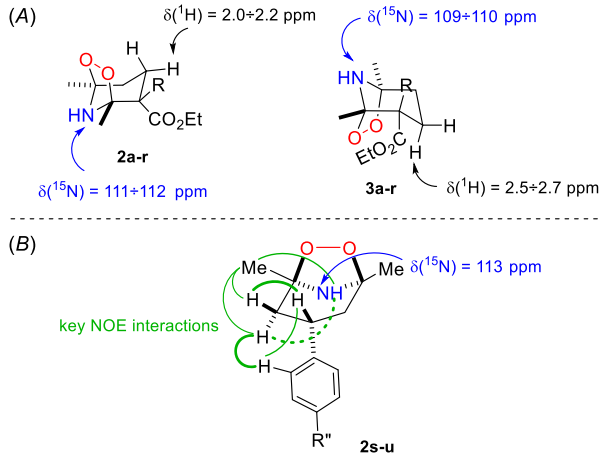

Figure 2. Basic ^{1}H, ^{15}N, and NOE NMR data for the stereochemical analysis of main types of the synthesized azaozonides **2a–u** and **3a–r**.

proton falls into the anisotropy cone of the C═O group and has a chemical shift (2.5–2.7 ppm) (Figure 2, A). The configuration of a single diastereomer of the 2-aryl-substituted azaozonides **2s–u** was established using $^{1}H–^{1}H$ NOESY spectra (Figure 2, B). The correctness of the performed assignments based on ^{1}H and ^{15}N chemical shifts was verified by a number of NOE data. NMR analysis of azaozonides was also facilitated by 2D correlation spectroscopic techniques (COSY, NOESY, editing-HSQC, and HMBC) that were previously calibrated by the NMR analysis of reference ozonides.

Interestingly, the ^{15}N NMR chemical shifts for the aminoperoxides are quite different from the chemical shifts for amines (49.6 and 39.1 ppm for diethylamine and piperidine, respectively; for the ^{15}N NMR spectra for amines see the SI) and are much closer to amides (106.4–108.4 and 102.2–104.2 ppm for *N*-methylformamide and *N*-methylacetamide, respectively[112]).

The NMR assignments were further confirmed by X-ray single-crystal analysis (Figure 3). A more detailed description

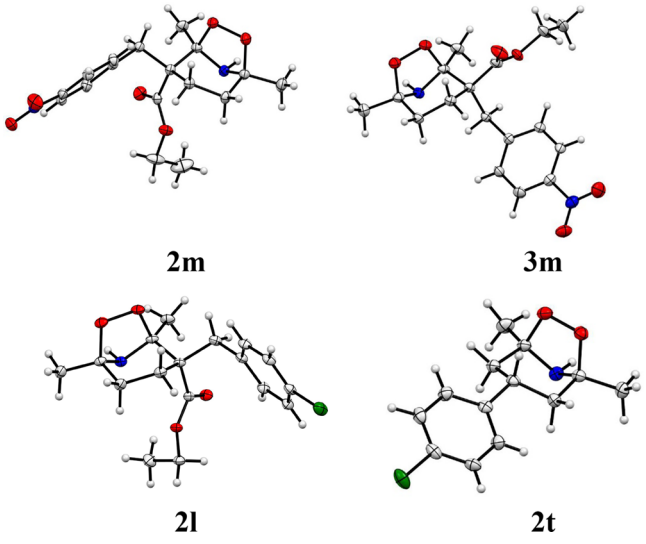

Figure 3. Molecular structures of **2l**, **2m**, **3m**, and **2t**. Atoms are presented as atomic displacement parameters (ADP) ellipsoids (50% probability).

of X-ray data for **2m**, **3m**, and **2t** is provided in the SI. An interesting feature of the amino group is that it is strongly pyramidalized in the direction that positions the lone pair of nitrogen antiperiplanar to the two C–O bonds of the peroxide ring. In the N-containing six-membered ring, the two C–O bonds to the peroxide moiety are axial, as expected from the generalized anomeric effect.[113–116]

Rearrangement of Bridged 1,2,4-Dioxazolidines (Bridged Azaozonides). Due to the high energy of peroxides, this functionality is prone to rearrangements. Because the O–O bond is generally the "weakest link" in the molecule, most of peroxide rearrangements proceed via O–O bond scission, as illustrated by Baeyer–Villiger, Criegee, Udris–Sergeev, Hock, Kornblum–DeLaMare, Wieland, and Story reactions.[122] Rearrangement of peroxides with preservation of the peroxide group is very rare. In fact, in the 100+ years of peroxide chemistry, only three such rearrangements are known, namely, the Schenck rearrangement,[117,118] the Smith rearrangement,[119] and an interconversion of stereoisomeric ozonides and tricyclic monoperoxides (Scheme 3)

Scheme 3. Currently Known Rearrangements of Peroxides That Preserve the Peroxide Group

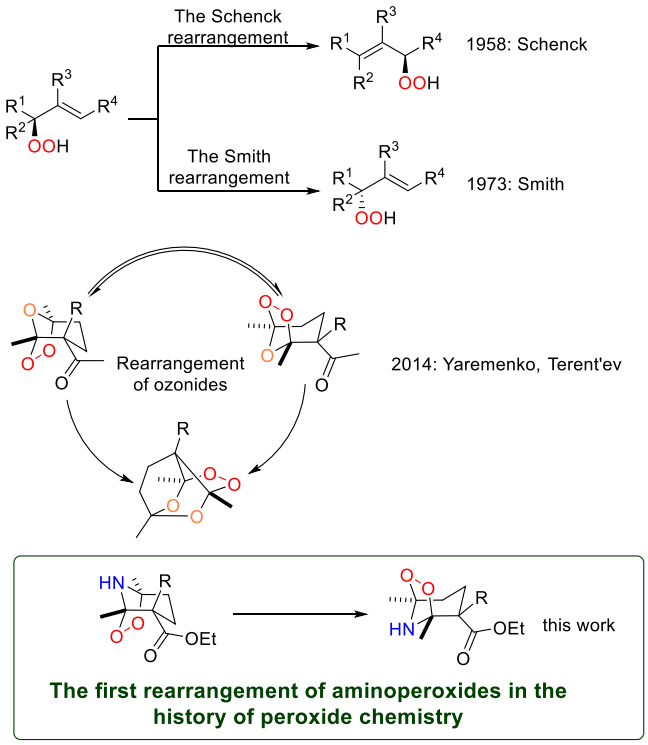

recently discovered by us.[120] Such "peroxide-conserving" rearrangements are exceptionally interesting from the fundamental point of view because they reveal kinetically favored reaction pathways far away from the thermodynamic minima. Generally, such pathways navigate the "high-altitude" regions of the potential energy surface and avoid falling down to the lowest energy "thermodynamic bottom". Such precise navigation is generally made possible by using stereoelectronically assisted activation that can selectively break the usually stronger (e.g., C–O) bonds in the presence of fragile O–O groups.

Our work describes *the first peroxide-preserving rearrangement of aminoperoxides in the history of peroxide chemistry.*

https://doi.org/10.1021/jacs.1c02249
J. Am. Chem. Soc. 2021, 143, 6634–6648

^{1}H NMR monitoring of the condensation of **1l** with H_2O_2 and aqueous NH_3 in CD_3OD demonstrated that the kinetically preferable azaozonide **3l** is thermodynamically less stable than its isomer **2l** (^{1}H NMR monitoring is presented in the SI). To confirm that azaozonides **3** can be rearranged into **2**, a 22% aqueous solution of NH_3 and 34% aqueous solution of H_2O_2 were added (in the same amounts as in run 6 of Table 1) to a solution of the mixtures of azaozonides **2h** + **3h**, **2k** + **3k**, or **2l** + **3l** in MeOH. The reaction mixtures were kept without stirring for 24 h at 20−25 °C. After that, the ratio of azaozonides **2h**:**3h** changed from 70:30 to 91:9, for **2k**:**3k** from 67:33 to 92:8, and for **2l**:**3l** from 35:65 to 96:4 (Scheme 4).

Scheme 4. Rearrangement of Azaozonides 3 into Azaozonides 2

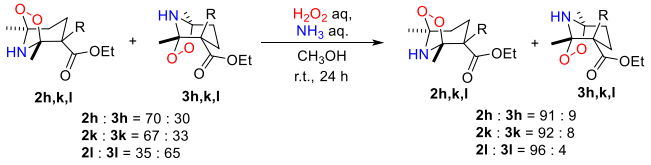

In the case of azaozonides **2l** + **3l**, colorless crystals of **2l** were formed. The X-ray structure of **2l** is shown in Figure 3. Also, the rearrangement of **3** into **2** can be realized by removing excess ammonia, hydrogen peroxide, and solvent on a rotary evaporator under vacuum of a membrane pump at 40−50 °C (under conditions of high concentrations of NH_3(aq) and H_2O_2(aq)). See the Computational Analysis section below for a probable mechanism of this rearrangement.

Stability of Bridged 1,2,4-Dioxazolidines (Bridged Azaozonides). All synthesized azaozonides **2a**−**u** and **3a**−**r** are stable compounds and can be stored at room temperature for several months without decomposition.

A pair of azaozonides **2l** and **3l** was used to study the stability of azaozonides with respect to 98% H_2SO_4, KOH, NH_3(aq), and NH_4OAc by NMR monitoring in CD_3OD with 1,4-dinitrobenzene as an internal standard (NMR spectra are presented in the SI). Azaozonides **2l** and **3l** were unstable toward H_2SO_4 (5 μL of 98% H_2SO_4 in 0.7 mL of CD_3OD per 50.0 mg of **2l** + **3l**). In 20 min after the addition of acid to the mixture of **2l** + **3l**, the decomposition of azaozonides **2l** and **3l** was observed (the content of azaozonides decreased by 42% and 89%, respectively), and after 24 h, the ^{1}H NMR signals characteristic of azaozonides disappeared. As a result, a complex mixture of products was formed where the initial diketone **1l** was also not detected. In the case of KOH, a decrease in the amount of azaozonides **2l** and **3l** was observed in 5 min after the KOH addition (by 12% and 17%, respectively). After 24 h, a further decrease in the amount of azaozonide **2l** was not observed while the amount of azaozonide **3l** decreased by 67% from the initial. Furthermore, azaozonide **2l** was resistant to NH_3(aq) and NH_4OAc. In contrast, azaozonide **3l** was found to be sensitive NH_3(aq) but less than that to NH_4OAc. In the case of NH_3(aq), the amount of azaozonide **3l** decreased by 35%, and in the case of NH_4OAc, by 70% from the initial after 24 h. Thus, azaozonide **2l** is resistant to KOH, NH_3(aq), and NH_4OAc and not resistant to H_2SO_4. Azaozonide **3l** is moderately resistant to NH_3(aq) but not resistant to H_2SO_4, KOH, and NH_4OAc.

The unusual stability of bridged azaperoxides under basic conditions opens the door for their modifications. A conceptually important feature of these reactions is that they represent the first transformations of azaperoxides that preserve the azaperoxide cycle (Scheme 5).

Scheme 5. Transformations of Azaperoxides 2h+3h with Preservation of the Peroxide Cycle

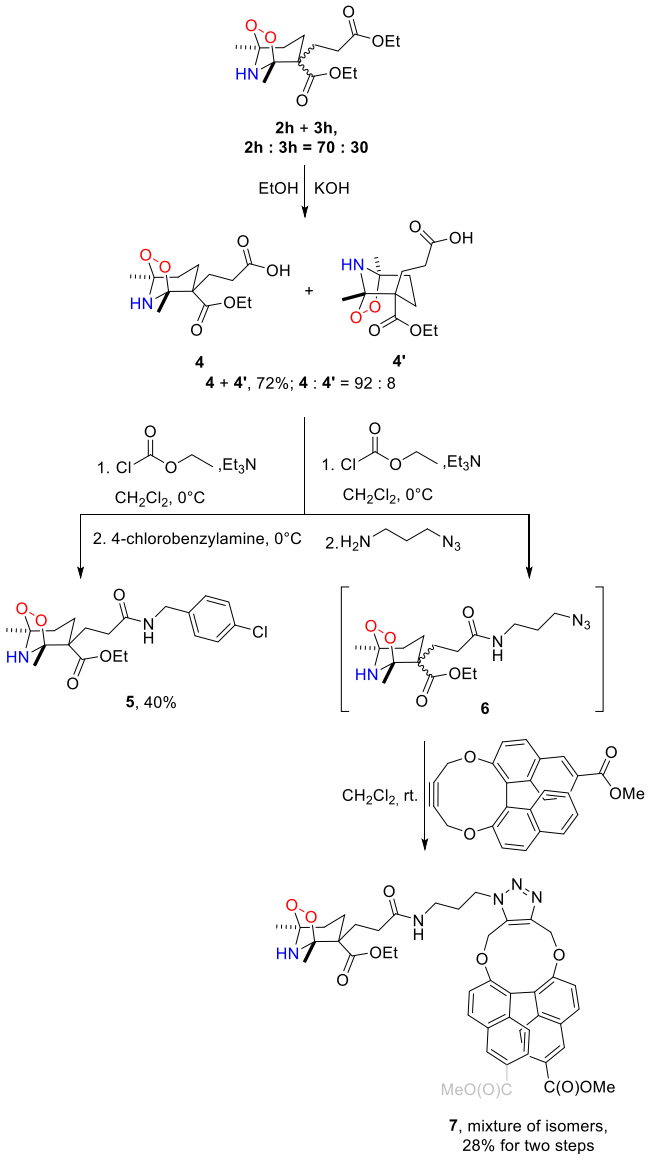

In particular, acid **4** formed from azaperoxides **2h**+**3h** can be used to prepare amides **5** and **6**. Note that the amine group in **2**/**3** does not react with the chloroformate. This is an unusual behavior for an unprotected secondary amine. Although isolation of azido-azaperoxide **6** is impractical, it can be used "as prepared" in a noncatalyzed click reaction with the formation of triazole-azaozonide **7** in 28% yield in two steps. The electronically activated[121] cycloalkyne partner for this reaction was synthesized according to the procedure of Harris et al.[122] in 55% yield.

COMPUTATIONAL ANALYSIS

All quantum chemical calculations were performed with the Gaussian16[123] program package at the PBE0[124]-D3BJ[125]/6-311++G(d,p)[126−129]/SMD[130](MeOH) level of theory. The

https://doi.org/10.1021/jacs.1c02249
J. Am. Chem. Soc. 2021, 143, 6634−6648

PBE0 functional is known to provide accurate results for organic reactions[131] and has been recently shown to be well grounded in theory.[132−134] All computational results are based on quasi-harmonically corrected free energies computed with GoodVibes.[126] Monte Carlo conformational search was performed for every computed intermediate and transition state; in the latter case the forming and breaking bonds were constrained at their lengths in a trial TS.[135] Stereoelectronic interactions were analyzed using natural bond orbital (NBO) analysis.[136] All energies are reported in kcal/mol.

Reaction Mechanism. To understand the mechanism of aminoperoxide formation from 1,5-diketones, we have modeled a variety of possible reaction pathways satisfying the experimental observations. For example, we have considered a route including the bicyclic ozonide (a close analogue of azaozonide obtained from the same ketones under acidic conditions and in the absence of NH_3[56,57]) as an intermediate. The negative Gibbs free energy for the transformation of ozonide to aminoperoxide demonstrates that this process is favorable thermodynamically (Scheme 6). Hence, the ozonide is a plausible intermediate in the assembly of the corresponding bicyclic aminoperoxide.

Scheme 6. Computed Free Energy of Transformation 15 → 3l in Reaction Media

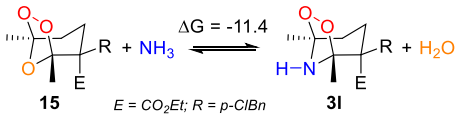

We have tested this scenario experimentally by introducing ozonide **15** into the reaction conditions of entry 11, Table 1 (Scheme 7). Formation of aminoperoxides **2l** and **3l** was not observed, and the ozonide remained unreacted. Thus, the kinetic barrier for the transformation **15** → **3** is too high to allow ozonides to be intermediates in the aminoperoxide formation under these experimental conditions.

Scheme 7. Attempt to Synthesize Aminoperoxides from Ozonides

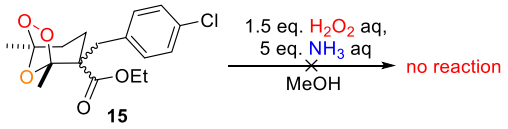

Modeling of the remaining reaction pathways for the formation of aminoperoxides (see SI) was performed using compound **1x**, a simplified version of **1a** with the CO_2Et group replaced with CO_2Me to decrease conformational flexibility. Analysis of the thermodynamic landscape involved interaction of the two nucleophiles (NH_3 and H_2O_2) with the two electrophilic centers of the diketone. The full network of possibilities (six distinct paths with 18 intermediates) is shown in the SI. The computationally favored path led us to the aminoperoxidation mechanism shown in Scheme 8. The reaction begins with nucleophilic addition of ammonia to a *β*-carbonyl group of the starting 1,5-diketone **1x**. Then it follows an intramolecular nucleophilic addition of the NH_2 group to the carbonyl group in intermediate **8x**, producing cyclic intermediate **9x**. This molecule undergoes a series of elimination/addition steps: first, a water molecule is eliminated from **9x** upon OH-group protonation, and then the resulting imine **10x** proceeds to nucleophilic addition of the H_2O_2 molecule from one of two sides. In order to close the second cycle, the formed intermediate (**11x** or **13x**) has to eliminate the remaining OH group, leading to an imine (**12x** or **14x**) that finally undergoes intramolecular nucleophilic attack of the imine carbon atom by the OOH group, resulting in the aminoperoxide **2** or **3**.

Scheme 8. Proposed Mechanism for the Assembly and Rearrangement of Aminoperoxides 2 and 3[a]

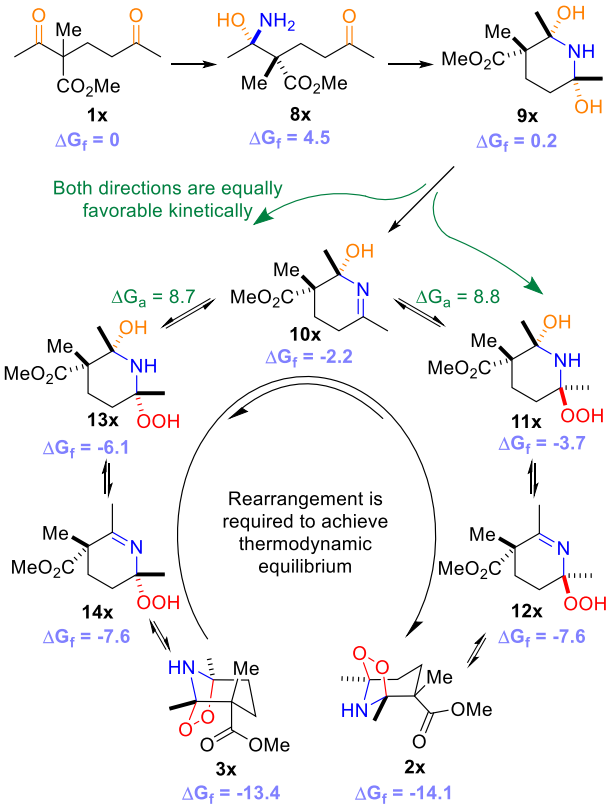

[a]All energies are reported in kcal/mol.

The computational analysis also offers a plausible mechanism for the observed rearrangement of aminoperoxides (Scheme 8). Alternative rearrangement mechanisms (see SI), which do not require H_2O_2 elimination, were found to be 3−5 kcal/mol higher in energy.

Transitions **10x** → **13x** and **10x** → **11x** have nearly identical barriers (8.7 and 8.8 kcal/mol). If the subsequent exergonic unimolecular steps in the parallel paths **10x** → **2x** and **10x** → **3x** are faster, one can expect that aminoperoxides **2x** and **3x** are formed in a 47:53 ratio (according to the Curtin−Hammett[137,138] equation at 25 °C), resulting in a system significantly shifted from the equilibrium 78:22 ratio (energy difference of 0.7 kcal/mol). This discrepancy between the kinetic and equilibrium ratios gives rise to the observed rearrangement. Since kinetic aminoperoxide **3x** is 11.2 kcal/mol more stable than **10x**, the energy barrier of rearrangement **3x** → **2x** is 11.2 kcal/mol higher than the barrier of **10x** → **2x** (i.e., 8.8 + 11.2 = 20.0 kcal/mol). This makes equilibration of the **2x**−**3x** mixture much slower than formation of aminoperoxides from the starting 1,5-diketone **1x**, in complete agreement with the experimental results: conversion of the

https://doi.org/10.1021/jacs.1c02249
J. Am. Chem. Soc. 2021, 143, 6634−6648

starting diketone into the initial mixture of **2l** and **3l** takes 1.5 h, while equilibrium is reached only after 36 h (see the SI).

It is also interesting to compare experimental equilibrium ratios **2a**:**3a** and **2l**:**3l** with the computed ones, **2x**:**3x** and **2l**:**3l**, under the assumption that the structural difference between **2a** and **2x** in a single CH_2 group does not influence selectivity significantly. The comparison in Scheme 9 shows surprisingly good correspondence between experimental and computational data.

Scheme 9. Experimental and Computational Equilibrium Ratios for Compounds 2 and 3

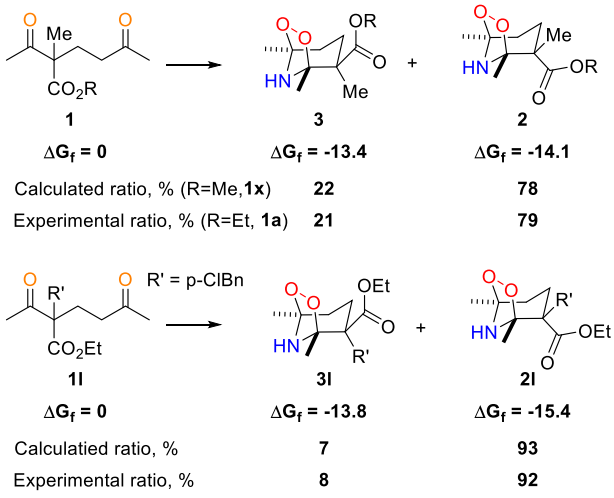

Stability and Electronic Structure of Bicyclic Azaozonides. Intrigued by the high stability and unusual features of these aminoperoxides, we have further explored their electronic structure. An isodesmic reaction constructed to highlight the difference between NH and O as neighbors for the peroxide group (Scheme 10) shows that NH is preferred

Scheme 10. Isodesmic Reaction Identifies the Amine Group as the Preferred Neighbor for the Peroxide Group

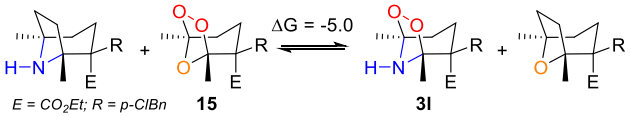

by 5 kcal/mol. The likely origin of this stability is the stronger anomeric interactions between the nitrogen lone pair and the C−O antibonding orbital.

Indeed, NBO analysis of a model aminoperoxide (Figure 4) shows that *each* of the above-mentioned $n_N \rightarrow \sigma^*_{C-O}$ interactions amounts to 12.2 kcal/mol, while its $n_O \rightarrow \sigma^*_{C-O}$ analogue in ozonides is only 9.1 kcal/mol.[57] In addition, moderate $n_O \rightarrow \sigma^*_{C-N}$ interaction amounts to 2.9 kcal/mol, a little less than the corresponding $n_O \rightarrow \sigma^*_{C-O}$ interaction in ozonides (3.4 kcal/mol[57]). Together, the anomeric interactions in an aminoperoxide add up to 37.6 kcal/mol vs 25 kcal/mol in ozonides.[57] Note that this difference in anomeric stabilization (12.6 kcal/mol) closely matches the overall energy difference between these compounds (11.4 kcal/mol, Scheme 6), highlighting the important role of hyperconjugative interactions in the stability of aminoperoxides.

However, it is also clear that the bicyclic structure of our aminoperoxides constrains their geometry in a way that

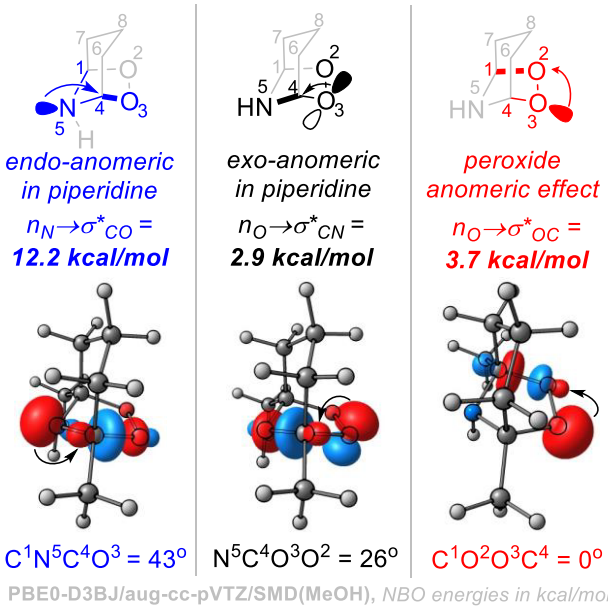

Figure 4. NBO analysis of aminoperoxides. Note that for this figure geometry optimizations and NBO calculations were performed using a larger, aug-cc-pVTZ[139] basis (see Figure S5 for more information).

prevents them from taking the full advantage of the nitrogen lone pair donor ability. As a reference point, it is instructive to compare the bicyclic azaozonides with hexamethylene triperoxide diamine,[140] one of the few known compounds containing geminal amine and peroxide groups. The latter compound has a remarkable molecular geometry (Figure 5)

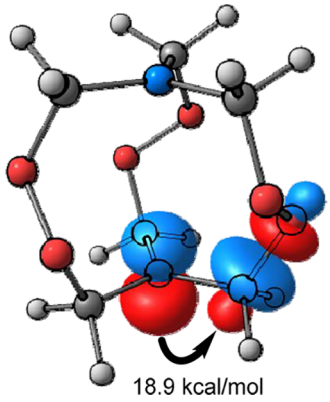

Figure 5. NBO analysis of hexamethylene triperoxide diamine optimized at the PBE0-D3BJ/6-311++G(d,p)/SMD(MeOH) level of theory.

where the amino groups are nearly planar, in contrast to the pyramidalized amino groups typical for amines.[141] Generally, the cost of planarization in amines is paid by the greater donor ability of nitrogen's pure-p lone pairs in delocalizing interactions.[142−144] In hexamethylene triperoxide diamine, the lone pair participates in three much stronger $n_N \rightarrow \sigma^*_{C-O}$ interactions (18.9 kcal/mol each, according to the NBO analysis). In our aminoperoxides, however, NBO analysis of the model compound found that planarization slightly weakens (by <1 kcal/mol) both the $n_N \rightarrow \sigma^*_{C-O}$ and the $n_O \rightarrow \sigma^*_{C-N}$ interactions (see Figure S5 for details) by misaligning the interacting orbitals. In the absence of greater delocalizing stabilization, the cost of planarization (9.9 kcal/mol) remains

https://doi.org/10.1021/jacs.1c02249
J. Am. Chem. Soc. 2021, 143, 6634−6648

about the same as in trimethylamine.[145] From a practical perspective, this analysis suggests that it should be possible to design even more anomerically deactivated amines by the future structural modifications.

More useful information from the NBO interaction energies is that the $n_N \rightarrow \sigma^*_{C-O}$ interactions are considerably stronger than the $n_O \rightarrow \sigma^*_{C-N}$ interactions (12.2 vs 2.9 × 2 kcal/mol). This situation indicates a relatively unbalanced pattern of delocalization where the nitrogen atom serves as a net donor toward the two peroxide oxygens. The imbalance is considerably more pronounced than in the case of the analogously coupled $n_N \rightarrow \sigma^*_{C-O}/n_O \rightarrow \sigma^*_{C-N}$ interactions in a hemiaminal (i.e., NR_2CH_2OR). It partially stems from the decreased donor ability of peroxide lone pairs ("the inverse α-effect"[116]) that we have identified recently as an important factor in peroxide chemistry.[146−150]

In order to further understand the interplay of structure and reactivity for the aminoperoxides **2l** and **3l**, the chemical properties of their NH groups were studied computationally in different roles, i.e., as bases, acids, and nucleophiles.

The nucleophilicity of **2l** was evaluated by comparing the activation barriers of its S_N2 reaction with methyl chloride with those for **2l_C** (its analogue with the peroxide fragment replaced with a CH_2-CH_2 group) and dimethylamine (see Scheme 11). The neighboring peroxide fragment increases the

Scheme 11. Activation Energies of S_N2 Reaction with Methyl Chloride Reveal Decreased Nucleophilicity of the Nitrogen Atom in Aminoperoxides

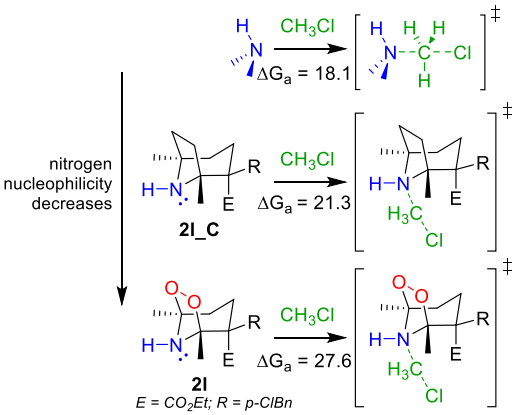

activation energy by 6−7 kcal/mol (**2l** vs **2l_C**), while embedding the NH group in the strained bicyclic system increases that by an additional 2−4 kcal/mol (**2l_C** vs dimethylamine). The latter observation can be traced to the increase of the nitrogen lone pair s-character caused by its strain-induced rehybridization in the polycyclic framework.[141] Together, these computational results agree with the experimentally observed inactivity of aminoperoxides **2**−**3l** toward alkylation with alkyl halides and acylation with acetyl chloride or acetic anhydride.

Trends in basicity (see Scheme 12) correlate with activation energies of S_N2 reactions and reveal another manifestation of the strong $n_N \rightarrow \sigma^*_{C-O}$ interaction in aminoperoxides. Protonation energies of aminoperoxides **2l** and **3l** are ∼18.5 kcal/mol higher than those for corresponding amines **2l_C** and **3l_C**. Thus, the peroxide group makes aminoperoxides less basic by ∼*15 pK_bunits*! This extremely large effect comes from

Scheme 12. Computed Energies of Protonation by NH_4^+ and Deprotonation by NH_3 in Reaction Media

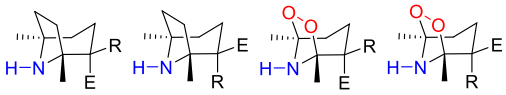

	2l_C	3l_C	2l	3l
Protonation ΔG, kcal/mol	2.6	3.1	21.1	21.5
Deprotonation ΔG, kcal/mol	46.1	43.7	31.0	29.8

E = CO_2Et; R = p-ClBn

NH-group basicity decreases
NH-group acidity increases

the penalty associated with the loss of $n_N \rightarrow \sigma^*_{C-O}$ interaction upon protonation.

Furthermore, the computed deprotonation energies show opposite trends in acidity, which illustrates the ability of the vicinal peroxide group to stabilize the negative charge on the nitrogen. Thus, the presence of vicinal peroxide deactivates the NH group's lone pair but simultaneously increases the N−H acidity.

The strong stereoelectronic interactions manifest themselves not only in reactivity but also in the NMR spectra. In the case of azaozonides, $n_N \rightarrow \sigma^*_{C-O}$ delocalization deshields the nitrogen atom, and, therefore, its ^{15}N NMR peak is expected to be shifted downfield. In order to estimate this deshielding, ^{15}N chemical shifts of **2l**, **2l_C**, and **2l′** (conformation of **2l′** with the N−H bond parallel to C−O) were computed using the GIAO method (see Scheme 13). According to calculations,

Scheme 13. ^{15}N Chemical Shifts Computed Using the GIAO Method at the PBE0-D3BJ/6-311++G(d,p)/SMD($CHCl_3$) Level of Theory[a]

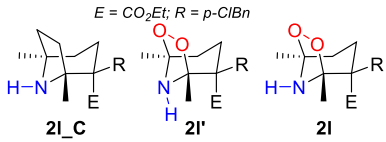

E = CO_2Et; R = p-ClBn

	2l_C	2l′	2l
^{15}N chemical shift, ppm	112.0	108.2	126.0

[a]Calculated chemical shift of NH_3 was used as the standard.

the nitrogen signal of **2l** is shifted downfield by 14−18 ppm away from the peaks of **2l_C** and **2l′**, where the $n_N \rightarrow \sigma^*_{C-O}$ hyperconjugation is "turned off". So, this interaction is indeed responsible for the deshielding of the nitrogen atom, and the unusual ^{15}N NMR chemical shifts in azaozonides can be taken as spectroscopic signatures of such stereoelectronic effects.

Another interesting feature of azaozonide reactivity is the difference between rates of **2l** and **3l** degradation in acidic media. Lower stability of **3l** against H_2SO_4 and SiO_2 was observed experimentally and was already mentioned in the synthetic section. Our calculations show that this difference comes from the closeness of peroxide oxygen to the ester side-group in **3l**. Computational analysis of protonated azaozonide **3l·H$^+$** and the corresponding TS reveals that the protonated ester group of **3l** acts as a proton donor for the peroxide group in the TS for C−O scission, thus stabilizing it and promoting the ring opening (Scheme 14).

The unusual behavior of the NH group in aminoperoxides can be useful for the medicinal chemistry of peroxides, since its

https://doi.org/10.1021/jacs.1c02249
J. Am. Chem. Soc. 2021, 143, 6634−6648

Scheme 14. Ring-Opening Activation Energies of Neutral and Protonated Forms of 3l in kcal/mol

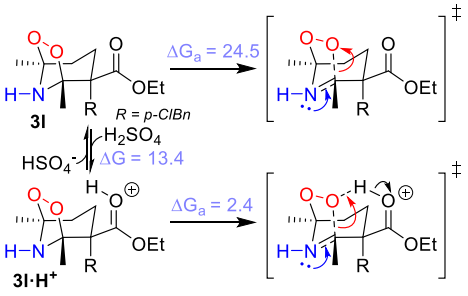

NH group does not interact with alkylating agents but can act as a strong H-bond donor when interacting with biosystems.

CONCLUSION

Stable bridged azaozonides are assembled via a catalyst-free three-component condensation of 1,5-diketones with hydrogen peroxide and an NH-group source such as aqueous ammonia, ammonium acetate, formate, or carbonate. This approach opens synthetic access to bridged azaozonides with various functional groups such as alkene, alkyne, ester, and cyano. The synthesis is readily scalable and opens practical access to gram quantities of the target azaozonides. The azaozonides can be stored at room temperature for several months without decomposition. They were isolated by ordinary column chromatography and fully characterized by NMR spectroscopy, mass spectrometry, X-ray, and elemental analysis. The first rearrangement in the class of aminoperoxides with preservation of the peroxide group was discovered. The stability of azaozonides was examined under acidic and basic conditions. The approach to azaozonides disclosed in this work makes this field of peroxide chemistry readily available for further exploration.

Computational analysis reveals that $n_N \rightarrow \sigma^*_{C-O}$ hyperconjugation is the key factor making NH a more favorable neighbor for the peroxide group than the oxygen atom, making azaozonides thermodynamically preferable over ozonides. The significant imbalance in the magnitude of $n_N \rightarrow \sigma^*_{C-O}$ and $n_O \rightarrow \sigma^*_{C-N}$ interactions between the amino and the peroxide groups is responsible for the unusually low basicity and nucleophilicity of azaozonides. This imbalance is amplified by the inverse α-effect, an important factor in peroxide reactivity. A combination of control experimental and computational analysis identified plausible mechanisms of the assembly and rearrangement of azaozonides. Interestingly, the two processes include the same intermediates: the rearrangement is driven by a difference in the kinetic and thermodynamic ratios of the azaozonide diastereomers.

ASSOCIATED CONTENT

Supporting Information

The Supporting Information is available free of charge at https://pubs.acs.org/doi/10.1021/jacs.1c02249.

Experimental details, characterization data, and quantum chemical calculations (PDF)
Computational data (XYZ)

Accession Codes

CCDC 2052452−2052454 and 2059164 contain the supplementary crystallographic data for this paper. These data can be obtained free of charge via www.ccdc.cam.ac.uk/data_request/cif, or by emailing data_request@ccdc.cam.ac.uk, or by contacting The Cambridge Crystallographic Data Centre, 12 Union Road, Cambridge CB2 1EZ, UK; fax: +44 1223 336033.

AUTHOR INFORMATION

Corresponding Authors

Ivan A. Yaremenko − *N. D. Zelinsky Institute of Organic Chemistry, Russian Academy of Sciences, 119991 Moscow, Russian Federation;* orcid.org/0000-0003-1068-9051; Email: yaremenko@ioc.ac.ru

Alexander O. Terent'ev − *N. D. Zelinsky Institute of Organic Chemistry, Russian Academy of Sciences, 119991 Moscow, Russian Federation;* orcid.org/0000-0001-8018-031X; Email: terentev@ioc.ac.ru

Igor V. Alabugin − *Department of Chemistry and Biochemistry, Florida State University, Tallahassee, Florida 32306, United States;* orcid.org/0000-0001-9289-3819; Email: alabugin@chem.fsu.edu

Authors

Yulia Yu. Belyakova − *N. D. Zelinsky Institute of Organic Chemistry, Russian Academy of Sciences, 119991 Moscow, Russian Federation*

Peter S. Radulov − *N. D. Zelinsky Institute of Organic Chemistry, Russian Academy of Sciences, 119991 Moscow, Russian Federation;* orcid.org/0000-0003-2653-0395

Roman A. Novikov − *N. D. Zelinsky Institute of Organic Chemistry, Russian Academy of Sciences, 119991 Moscow, Russian Federation;* orcid.org/0000-0002-3740-7424

Michael G. Medvedev − *N. D. Zelinsky Institute of Organic Chemistry, Russian Academy of Sciences, 119991 Moscow, Russian Federation;* orcid.org/0000-0001-7070-4052

Nikolai V. Krivoshchapov − *N. D. Zelinsky Institute of Organic Chemistry, Russian Academy of Sciences, 119991 Moscow, Russian Federation*

Alexander A. Korlyukov − *A. N. Nesmeyanov Institute of Organoelement Compounds, Russian Academy of Sciences, 119991 Moscow, Russian Federation;* orcid.org/0000-0002-5600-9886

Complete contact information is available at: https://pubs.acs.org/10.1021/jacs.1c02249

Notes

The authors declare no competing financial interest.

ACKNOWLEDGMENTS

A.O.T., I.A.Y., Y.Y.B., P.S.R., R.A.N., M.G.M., N.V.K., and A.A.K. are grateful for the support of the Russian Science Foundation (Grant No. 21-43-04417). Quantum chemical calculations have been carried out using computing resources of the federal collective usage center Complex for Simulation and Data Processing for Mega-science Facilities at NRC "Kurchatov Institute", http://ckp.nrcki.ru/. The Siberian Branch of the Russian Academy of Sciences (SB RAS) Siberian Supercomputer Center is gratefully acknowledged for providing supercomputer facilities. The research is carried out using the equipment of the shared research facilities of HPC computing resources at Lomonosov Moscow State University.[51] The authors acknowledge the computational resources provided by the Moscow State University's Faculty of Computational Mathematics and Cybernetics (IBM Blue

https://doi.org/10.1021/jacs.1c02249
J. Am. Chem. Soc. 2021, 143, 6634−6648

Gene/P, Polus). I.V.A. is grateful to the National Science Foundation for the financial support at FSU (CHE-1800329).

REFERENCES

(1) Fisher, L. C.; Blackie, M. A. L. Tetraoxanes as Antimalarials: Harnessing the Endoperoxide. *Mini-Rev. Med. Chem.* **2014**, *14* (2), 123−135.
(2) Ghorai, P.; Dussault, P. H.; Hu, C. Synthesis of Spirobisperoxyketals. *Org. Lett.* **2008**, *10* (12), 2401−2404.
(3) Hao, H. D.; Wittlin, S.; Wu, Y. Potent Antimalarial 1,2,4-Trioxanes through Perhydrolysis of Epoxides. *Chem. - Eur. J.* **2013**, *19* (23), 7605−7619.
(4) Šolaja, B. A.; Terzić, N.; Pocsfalvi, G.; Gerena, L.; Tinant, B.; Opsenica, D.; Milhous, W. K. Mixed Steroidal 1,2,4,5-Tetraoxanes: Antimalarial and Antimycobacterial Activity. *J. Med. Chem.* **2002**, *45* (16), 3331−3336.
(5) Jefford, C. W. Synthetic Peroxides as Potent Antimalarials. News and Views. *Curr. Top. Med. Chem.* **2012**, *12* (5), 373−399.
(6) Wang, X.; Dong, Y.; Wittlin, S.; Charman, S. A.; Chiu, F. C. K.; Chollet, J.; Katneni, K.; Mannila, J.; Morizzi, J.; Ryan, E.; Scheurer, C.; Steuten, J.; Santo Tomas, J.; Snyder, C.; Vennerstrom, J. L. Comparative Antimalarial Activities and ADME Profiles of Ozonides (1,2,4-trioxolanes) OZ277, OZ439, and Their 1,2-Dioxolane, 1,2,4-Trioxane, and 1,2,4,5-Tetraoxane Isosteres. *J. Med. Chem.* **2013**, *56* (6), 2547−2555.
(7) Chaudhari, M. B.; Mohanta, N.; Pandey, A. M.; Vandana, M.; Karmodiya, K.; Gnanaprakasam, B. Peroxidation of 2-oxindole and barbituric acid derivatives under batch and continuous flow using an eco-friendly ethyl acetate solvent. *React. Chem. Eng.* **2019**, *4* (7), 1277−1283.
(8) Giannangelo, C.; Fowkes, F. J. I.; Simpson, J. A.; Charman, S. A.; Creek, D. J. Ozonide Antimalarial Activity in the Context of Artemisinin-Resistant Malaria. *Trends Parasitol.* **2019**, *35* (7), 529−543.
(9) Xiao, J.; Sun, Z.; Kong, F.; Gao, F. Current scenario of ferrocene-containing hybrids for antimalarial activity. *Eur. J. Med. Chem.* **2020**, *185*, 111791.
(10) Boissier, J.; Portela, J.; Pradines, V.; Coslédan, F.; Robert, A.; Meunier, B. Activity of trioxaquine PA1259 in mice infected by Schistosoma mansoni. *C. R. Chim.* **2012**, *15* (1), 75−78.
(11) Ingram, K.; Yaremenko, I. A.; Krylov, I. B.; Hofer, L.; Terent'ev, A. O.; Keiser, J. Identification of Antischistosomal Leads by Evaluating Bridged 1,2,4,5-Tetraoxanes, Alphaperoxides, and Tricyclic Monoperoxides. *J. Med. Chem.* **2012**, *55* (20), 8700−8711.
(12) Keiser, J.; Ingram, K.; Vargas, M.; Chollet, J.; Wang, X.; Dong, Y.; Vennerstrom, J. L. In Vivo Activity of Aryl Ozonides against Schistosoma Species. *Antimicrob. Agents Chemother.* **2012**, *56* (2), 1090.
(13) Keiser, J.; Veneziano, V.; Rinaldi, L.; Mezzino, L.; Duthaler, U.; Cringoli, G. Anthelmintic activity of artesunate against Fasciola hepatica in naturally infected sheep. *Res. Vet. Sci.* **2010**, *88* (1), 107−110.
(14) Küster, T.; Kriegel, N.; Stadelmann, B.; Wang, X.; Dong, Y.; Vennerstrom, J. L.; Keiser, J.; Hemphill, A. Amino ozonides exhibit in vitro activity against Echinococcus multilocularis metacestodes. *Int. J. Antimicrob. Agents* **2014**, *43* (1), 40−46.
(15) Cabral, L. I. L.; Pomel, S.; Cojean, S.; Amado, P. S. M.; Loiseau, P. M.; Cristiano, M. L. S., Synthesis and Antileishmanial Activity of 1,2,4,5-Tetraoxanes against Leishmania donovani. *Molecules* **2020**, *25* (3), 465.
(16) Abrams, R. P.; Carroll, W. L.; Woerpel, K. A. Five-Membered Ring Peroxide Selectively Initiates Ferroptosis in Cancer Cells. *ACS Chem. Biol.* **2016**, *11* (5), 1305−1312.
(17) Alagbala, A. A.; McRiner, A. J.; Borstnik, K.; Labonte, T.; Chang, W.; D'Angelo, J. G.; Posner, G. H.; Foster, B. A. Biological Mechanisms of Action of Novel C-10 Non-Acetal Trioxane Dimers in Prostate Cancer Cell Lines. *J. Med. Chem.* **2006**, *49* (26), 7836−7842.
(18) Chaturvedi, D.; Goswami, A.; Pratim Saikia, P.; Barua, N. C.; Rao, P. G. Artemisinin and its derivatives: a novel class of anti-malarial and anti-cancer agents. *Chem. Soc. Rev.* **2010**, *39* (2), 435−454.
(19) Chaudhari, M. B.; Moorthy, S.; Patil, S.; Bisht, G. S.; Mohamed, H.; Basu, S.; Gnanaprakasam, B. Iron-Catalyzed Batch/Continuous Flow C−H Functionalization Module for the Synthesis of Anticancer Peroxides. *J. Org. Chem.* **2018**, *83* (3), 1358−1368.
(20) Chen, H.-H.; Zhou, H.-J.; Wang, W.-Q.; Wu, G.-D. J. C. C. Pharmacology, Antimalarial dihydroartemisinin also inhibits angiogenesis. *Cancer Chemother. Pharmacol.* **2004**, *53* (5), 423−432.
(21) Coghi, P.; Yaremenko, I. A.; Prommana, P.; Radulov, P. S.; Syroeshkin, M. A.; Wu, Y. J.; Gao, J. Y.; Gordillo, F. M.; Mok, S.; Wong, V. K. W.; Uthaipibull, C.; Terent'ev, A. O. Novel Peroxides as Promising Anticancer Agents with Unexpected Depressed Antimalarial Activity. *ChemMedChem* **2018**, *13* (9), 902−908.
(22) Dwivedi, A.; Mazumder, A.; du Plessis, L.; du Preez, J. L.; Haynes, R. K.; du Plessis, J. In vitro anti-cancer effects of artemisone nano-vesicular formulations on melanoma cells. *Nanomedicine* **2015**, *11* (8), 2041−2050.
(23) Rubush, D. M.; Morges, M. A.; Rose, B. J.; Thamm, D. H.; Rovis, T. An Asymmetric Synthesis of 1,2,4-Trioxane Anticancer Agents via Desymmetrization of Peroxyquinols through a Brønsted Acid Catalysis Cascade. *J. Am. Chem. Soc.* **2012**, *134* (33), 13554−13557.
(24) Yaremenko, I. A.; Coghi, P.; Prommana, P.; Qiu, C.; Radulov, P. S.; Qu, Y.; Belyakova, Y. Y.; Zanforlin, E.; Kokorekin, V. A.; Wu, Y. Y. J.; Fleury, F.; Wong, V. K. W.; Uthaipibull, C.; Terent'ev, A. Synthetic peroxides promote apoptosis of cancer cells inhibiting of P-glycoprotein ABCB5. *ChemMedChem* **2020**, *15* (13), 1118−1127.
(25) Gao, F.; Sun, Z.; Kong, F.; Xiao, J. Artemisinin-derived hybrids and their anticancer activity. *Eur. J. Med. Chem.* **2020**, *188*, 112044.
(26) Vil', V. A.; Yaremenko, I. A.; Fomenkov, D. I.; Levitsky, D. O.; Fleury, F.; Terent'ev, A. O. Ion exchange resin-catalyzed synthesis of bridged tetraoxanes possessing in vitro cytotoxicity against HeLa cancer cells. *Chem. Heterocycl. Compd.* **2020**, *56* (6), 722−726.
(27) Yaremenko, I. A.; Syromyatnikov, M. Y.; Radulov, P. S.; Belyakova, Y. Y.; Fomenkov, D. I.; Popov, V. N.; Terent'ev, A. O. Cyclic Synthetic Peroxides Inhibit Growth of Entomopathogenic Fungus Ascosphaera apis without Toxic Effect on Bumblebees. *Molecules* **2020**, *25* (8), 1954.
(28) Chaudhary, S.; Sharma, V.; Jaiswal, P. K.; Gaikwad, A. N.; Sinha, S. K.; Puri, S. K.; Sharon, A.; Maulik, P. R.; Chaturvedi, V. Stable Tricyclic Antitubercular Ozonides Derived from Artemisinin. *Org. Lett.* **2015**, *17* (20), 4948−4951.
(29) Miller, M. J.; Walz, A. J.; Zhu, H.; Wu, C.; Moraski, G.; Möllmann, U.; Tristani, E. M.; Crumbliss, A. L.; Ferdig, M. T.; Checkley, L.; Edwards, R. L.; Boshoff, H. I. Design, Synthesis, and Study of a Mycobactin−Artemisinin Conjugate That Has Selective and Potent Activity against Tuberculosis and Malaria. *J. Am. Chem. Soc.* **2011**, *133* (7), 2076−2079.
(30) Zhou, F.-W.; Lei, H.-S.; Fan, L.; Jiang, L.; Liu, J.; Peng, X.-M.; Xu, X.-R.; Chen, L.; Zhou, C.-H.; Zou, Y.-Y.; Liu, C.-P.; He, Z.-Q.; Yang, D.-C. Design, synthesis, and biological evaluation of dihydroartemisinin−fluoroquinolone conjugates as a novel type of potential antitubercular agents. *Bioorg. Med. Chem. Lett.* **2014**, *24* (8), 1912−1917.
(31) Chou, S. W.; Marousek, G.; Auerochs, S.; Stamminger, T.; Milbradt, J.; Marschall, M. The unique antiviral activity of artesunate is broadly effective against human cytomegaloviruses including therapy-resistant mutants. *Antiviral Res.* **2011**, *92* (2), 364−368.
(32) Efferth, T.; Romero, M. R.; Wolf, D. G.; Stamminger, T.; Marin, J. J. G.; Marschall, M. The antiviral activities of artemisinin and artesunate. *Clin. Infect. Dis.* **2008**, *47* (6), 804−811.
(33) Reiter, C.; Frohlich, T.; Gruber, L.; Hutterer, C.; Marschall, M.; Voigtlander, C.; Friedrich, O.; Kappes, B.; Efferth, T.; Tsogoeva, S. B. Highly potent artemisinin-derived dimers and trimers: Synthesis and evaluation of their antimalarial, antileukemia and antiviral activities. *Bioorg. Med. Chem.* **2015**, *23* (17), 5452−5458.

https://doi.org/10.1021/jacs.1c02249
J. Am. Chem. Soc. 2021, 143, 6634−6648

(34) Shah, A., Mateon Expands its COVID-19 Therapeutic Program to include Artemisinin. www.biospace.com/article/releases/mateon-expands-its-covid-19-therapeutic-program-to-include-artemisinin 2020 (access date Oct 18, 2020).
(35) Li, S.-y.; Chen, C.; Zhang, H.-q.; Guo, H.-y.; Wang, H.; Wang, L.; Zhang, X.; Hua, S.-n.; Yu, J.; Xiao, P.-g.; Li, R.-s.; Tan, X. Identification of natural compounds with antiviral activities against SARS-associated coronavirus. *Antiviral Res.* **2005**, *67* (1), 18−23.
(36) Yang, Y.; Islam, M. S.; Wang, J.; Li, Y.; Chen, X. Traditional Chinese Medicine in the Treatment of Patients Infected with 2019-New Coronavirus (SARS-CoV-2): A Review and Perspective. *Int. J. Biol. Sci.* **2020**, *16* (10), 1708−1717.
(37) Dembitsky, V. M.; Yaremenko, I. A. Stable and Unstable 1,2-Dioxolanes: Origin, Synthesis, and Biological Activities. In *Knowledge Updates 2020/2*; Georg Thieme Verlag: Stuttgart, 2020; pp 277−314.
(38) Ibrahim, S. R. M.; Ebel, R.; Wray, V.; Mueller, W. E. G.; Edrada-Ebel, R.; Proksch, P. Diacarperoxides, norterpene cyclic peroxides from the sponge Diacarnus megaspinorhabdosa. *J. Nat. Prod.* **2008**, *71* (8), 1358−1364.
(39) Norris, M. D.; Perkins, M. V. Structural diversity and chemical synthesis of peroxide and peroxide-derived polyketide metabolites from marine sponges. *Nat. Prod. Rep.* **2016**, *33* (7), 861−880.
(40) Tokuyasu, T.; Kunikawa, S.; Masuyama, A.; Nojima, M. Co(III)-alkyl complex- and Co(III)-alkylperoxo complex-catalyzed triethylsilylperoxidation of alkenes with molecular oxygen and triethylsilane. *Org. Lett.* **2002**, *4* (21), 3595−3598.
(41) Dai, P.; Dussault, P. H. Intramolecular reactions of hydroperoxides and oxetanes: Stereoselective synthesis of 1,2-dioxolanes and 1,2-dioxanes. *Org. Lett.* **2005**, *7* (20), 4333−4335.
(42) Ramirez, A.; Woerpel, K. A. Synthesis of 1,2-dioxolanes by annulation reactions of peroxycarbenium ions with alkenes. *Org. Lett.* **2005**, *7* (21), 4617−4620.
(43) Tokuyasu, T.; Kunikawa, S.; McCullough, K. J.; Masuyama, A.; Nojima, M. Synthesis of cyclic peroxides by chemo- and regioselective peroxidation of dienes with Co(II)/O-2/Et3SiH. *J. Org. Chem.* **2005**, *70* (1), 251−260.
(44) Tsubusaki, T.; Nishino, H. Formation of 1,2-dioxolanes using Mn(III)-based reaction of various arylacetylenes with 2,4-pentanedione and related reaction. *Tetrahedron* **2009**, *65* (18), 3745−3752.
(45) Li, Y.; Wittlin, S.; Wu, Y. K. Antimalarial Spiro-Bridged 1,2-Dioxolanes Via Intramolecular Addition of Peroxycarbenium Ions to C-C Double Bonds. *Heterocycles* **2012**, *86* (1), 245−254.
(46) Hurlocker, B.; Miner, M. R.; Woerpel, K. A. Synthesis of Silyl Monoperoxyketals by Regioselective Cobalt-Catalyzed Peroxidation of Silyl Enol Ethers: Application to the Synthesis of 1,2-Dioxolanes. *Org. Lett.* **2014**, *16* (16), 4280−4283.
(47) Kandur, W. V.; Richert, K. J.; Rieder, C. J.; Thomas, A. M.; Hu, C. H.; Ziller, J. W.; Woerpel, K. A. Synthesis and Reactivity of 1,2-Dioxolanes from beta,gamma-Epoxy Ketones. *Org. Lett.* **2014**, *16* (10), 2650−2653.
(48) Nguyen, T. L.; Ferrie, L.; Figadere, B. Synthesis of 3,5-disubstituted-1,2-dioxolanes: access to analogues of mycangimycin and some rearrangement products. *Tetrahedron Lett.* **2016**, *57* (47), 5286−5289.
(49) Xu, Z. J.; Wittlin, S.; Wu, Y. K. Probing the Peroxycarbenium [3 + 2] Cycloaddition Reactions with 1,2-Disubstituted Ethylenes: Results and Insights. *Chem. - Eur. J.* **2017**, *23* (9), 2031−2034.
(50) Cabrera-Afonso, M. J.; Lucena, S. R.; Juarranz, A.; Urbano, A.; Carreno, M. C. Selective Oxidative Dearomatization of Angular Tetracyclic Phenols by Controlled Irradiation under Air: Synthesis of an Angucyclinone-Type Double Peroxide with Anticancer Properties. *Org. Lett.* **2018**, *20* (19), 6094−6098.
(51) Criegee, R.; Lohaus, G. Über das Ozonid des 1.2-Dimethyl-cyclopentens-(1) (II. Mitteil. über den Verlauf der Ozonspaltung). *Chem. Ber.* **1953**, *86* (1), 1−4.
(52) Kondelíková, J.; Králíček, J.; Kubánek, V. Reactions of 2,2'-methylene-bis(cyclohexanone) with hydrogen peroxide and peroxy acids. *Collect. Czech. Chem. Commun.* **1972**, *37*, 263−269.
(53) Griesbaum, K.; Liu, X.; Kassiaris, A.; Scherer, M. Ozonolyses of O-Alkylated Ketoximes in the Presence of Carbonyl Groups: A Facile Access to Ozonides. *Liebigs Ann.* **1997**, *1997* (7), 1381−1390.
(54) Griesbaum, K.; Miclaus, V.; Jung, I. C.; Quinkert, R.-O. Gas-Phase Reactions of 1,2-Dimethylcyclopentene and of 2,6-Heptanedione with Ozone: Unprecedented Formation of an Ozonide by Ozone Treatment of a Diketone. *Eur. J. Org. Chem.* **1998**, *1998* (4), 627−629.
(55) Kvasnica, M.; Tišlerová, I.; Šarek, J.; Sejbal, J.; Císařová, I. Preparation of New Oxidized 18-α-Oleanane Derivatives. *Collect. Czech. Chem. Commun.* **2005**, *70*, 1447−1464.
(56) Gomes, G. D.; Yaremenko, I. A.; Radulov, P. S.; Novikov, R. A.; Chernyshev, V. V.; Korlyukov, A. A.; Nikishin, G. I.; Alabugin, I. V.; Terent'ev, A. O. Stereoelectronic Control in the Ozone-Free Synthesis of Ozonides. *Angew. Chem., Int. Ed.* **2017**, *56* (18), 4955−4959.
(57) Yaremenko, I. A.; Gomes, G. D.; Radulov, P. S.; Belyakova, Y. Y.; Vilikotskiy, A. E.; Vil', V. A.; Korlyukov, A. A.; Nikishin, G. I.; Alabugin, I. V.; Terent'ev, A. O. Ozone-Free Synthesis of Ozonides: Assembling Bicyclic Structures from 1,5-Diketones and Hydrogen Peroxide. *J. Org. Chem.* **2018**, *83* (8), 4402−4426.
(58) Akimova, T. I.; Rybin, V. G.; Soldatkina, O. A. New Tetracyclic Spiro-1,2,4-trioxolanes (Ozonides). Synthesis and Mass Spectrometric Study. *Russ. J. Org. Chem.* **2019**, *55* (1), 101−107.
(59) Dussault, P. H.; Davies, D. R. Synthesis of 1,2-dioxanes, 1,2,4-trioxanes, and 1,2,4-trioxepanes via cyclizations of unsaturated hydroperoxyacetals. *Tetrahedron Lett.* **1996**, *37* (4), 463−466.
(60) Gemma, S.; Martí, F.; Gabellieri, E.; Campiani, G.; Novellino, E.; Butini, S. Synthetic studies toward 1,2-dioxanes as precursors of potential endoperoxide-containing antimalarials. *Tetrahedron Lett.* **2009**, *50* (41), 5719−5722.
(61) Xu, C.; Schwartz, C.; Raible, J.; Dussault, P. H. Asymmetric synthesis of 1,2-dioxanes: approaches to the peroxyplakoric acids. *Tetrahedron* **2009**, *65* (47), 9680−9685.
(62) Daeppen, C.; Kaiser, M.; Neuburger, M.; Gademann, K. Preparation of Antimalarial Endoperoxides by a Formal [2 + 2 + 2] Cycloaddition. *Org. Lett.* **2015**, *17* (21), 5420−5423.
(63) Hu, L.; Lu, X.; Deng, L. Catalytic Enantioselective Peroxidation of α,β-Unsaturated Aldehydes for the Asymmetric Synthesis of Biologically Important Chiral Endoperoxides. *J. Am. Chem. Soc.* **2015**, *137* (26), 8400−8403.
(64) Novkovic, L.; Trmcic, M.; Rodic, M.; Bihelovic, F.; Zlatar, M.; Matovic, R.; Saicic, R. N. Synthesis of endoperoxides by domino reactions of ketones and molecular oxygen. *RSC Adv.* **2015**, *5* (120), 99577−99584.
(65) Zhang, Q.; Jin, H.-X.; Wu, Y. A facile access to bridged 1,2,4-trioxanes. *Tetrahedron* **2006**, *62* (50), 11627−11634.
(66) Ramirez, A. P.; Thomas, A. M.; Woerpel, K. A. Preparation of Bicyclic 1,2,4-Trioxanes from γ,δ-Unsaturated Ketones. *Org. Lett.* **2009**, *11* (3), 507−510.
(67) Griesbeck, A. G.; Schlundt, V. 5-Adamantylated 1,2,4-Trioxanes: Adamantane Position is Crucial for Antiparasitic Activity. *Synlett* **2011**, *2011* (16), 2430−2432.
(68) Zhang, M.; Han, Y.; Niu, J.-L.; Zhang, Z.-H. A General and Practical Approach for the Synthesis of 1,2,4-Trioxanes Catalyzed by Silica-Ferric Chloride. *Adv. Synth. Catal.* **2017**, *359* (20), 3618−3625.
(69) Riveira, M. J.; Martiren, N. L.; Mischne, M. P. Domino Self-Sensitized Photooxygenation of Conjugated Dienones for the Synthesis of 1,2,4-Trioxanes. *J. Org. Chem.* **2019**, *84* (6), 3671−3677.
(70) Ghorai, P.; Dussault, P. H. Broadly Applicable Synthesis of 1,2,4,5-Tetraoxanes. *Org. Lett.* **2009**, *11* (1), 213−216.
(71) Yan, X.; Chen, J.; Zhu, Y.-T.; Qiao, C. Phosphomolybdic Acid Catalyzed Synthesis of 1,2,4,5-Tetraoxanes. *Synlett* **2011**, *2011* (19), 2827−2830.
(72) Terent'ev, A. O.; Yaremenko, I. A.; Vil', V. A.; Moiseev, I. K.; Kon'kov, S. A.; Dembitsky, V. M.; Levitsky, D. O.; Nikishin, G. I. Phosphomolybdic and phosphotungstic acids as efficient catalysts for the synthesis of bridged 1,2,4,5-tetraoxanes from β-diketones and hydrogen peroxide. *Org. Biomol. Chem.* **2013**, *11* (16), 2613−2623.

https://doi.org/10.1021/jacs.1c02249
J. Am. Chem. Soc. 2021, 143, 6634−6648

(73) Radulov, P. S.; Belyakova, Y. Y.; Demina, A. A.; Nikishin, G. I.; Yaremenko, I. A.; Terent'ev, A. O. Selective synthesis of cyclic triperoxides from 1,1-dihydroperoxydi(cycloalkyl)peroxides and acetals using SnCl4. *Russ. Chem. Bull.* **2019**, *68* (6), 1289−1292.
(74) Terent'ev, A. O.; Yaremenko, I. A.; Glinushkin, A. P.; Nikishin, G. I. Synthesis of peroxides from *β,δ*-triketones under heterogeneous conditions. *Russ. J. Org. Chem.* **2015**, *51* (12), 1681−1687.
(75) Terent'ev, A. O.; Yaremenko, I. A.; Vil', V. A.; Dembitsky, V. M.; Nikishin, G. I. Boron Trifluoride as an Efficient Catalyst for the Selective Synthesis of Tricyclic Monoperoxides from beta,delta-Triketones and H2O2. *Synthesis* **2013**, *45* (2), 246−250.
(76) Radulov, P. S.; Yaremenko, I. A. Application of BF3 center dot Et2O in the synthesis of cyclic organic peroxides. *Chem. Heterocycl. Compd.* **2020**, *56* (9), 1146−1148.
(77) Cole, R. J.; Kirksey, J. W.; Moore, J. H.; Blankenship, B. R.; Diener, U. L.; Davis, N. D. Tremorgenic toxin from Penicillium veruculosum. *Appl. Microbiol.* **1972**, *24* (2), 248−250.
(78) Cole, R. J.; Kirksey, J. W. Mycotoxin verruculogen. 6-O-Methylindole. *J. Agric. Food Chem.* **1973**, *21* (5), 927−929.
(79) Cole, R. J.; Kirksey, J. W.; Cox, R. H.; Clardy, J. Structure of the tremor-producing indole, TR-2. *J. Agric. Food Chem.* **1975**, *23* (5), 1015−1018.
(80) Yoshizawa, T.; Morooka, N.; Sawada, Y.; Udagawa, S.-I. Tremorgenic Mycotoxin from Penicillium paraherquei. *Appl. Environ. Microbiol.* **1976**, *32* (3), 441−442.
(81) Fayos, J.; Lokensgard, D.; Clardy, J.; Cole, R. J.; Kirksey, J. W. Structure of verruculogen, a tremor producing peroxide from Penicillium verruculosum. *J. Am. Chem. Soc.* **1974**, *96* (21), 6785−6787.
(82) Yamazaki, M.; Suzuki, S.; Miyaki, K. Tremorgenic toxins from Aspergillus fumigatus Fres. *Chem. Pharm. Bull.* **1971**, *19* (8), 1739−1740.
(83) Yamazaki, M.; Fujimoto, H.; Kawasaki, T. Chemistry of tremorogenic metabolites. I. Fumitremorgin A from Aspergillus fumigatus. *Chem. Pharm. Bull.* **1980**, *28* (1), 245−254.
(84) Feng, Y.; Holte, D.; Zoller, J.; Umemiya, S.; Simke, L. R.; Baran, P. S. Total Synthesis of Verruculogen and Fumitremorgin A Enabled by Ligand-Controlled C-H Borylation. *J. Am. Chem. Soc.* **2015**, *137* (32), 10160−10163.
(85) Harmse, R.; Coertzen, D.; Wong, H. N.; Smit, F. J.; van der Watt, M. E.; Reader, J.; Nondaba, S. H.; Birkholtz, L. M.; Haynes, R. K.; N'Da, D. D. Activities of 11-Azaartemisinin and N-Sulfonyl Derivatives against Asexual and Transmissible Malaria Parasites. *ChemMedChem* **2017**, *12* (24), 2086−2093.
(86) Le, T. N.; De Borggraeve, W. M.; Grellier, P.; Pham, V. C.; Dehaen, W.; Nguyen, V. H. Synthesis of 11-aza-artemisinin derivatives using the Ugi reaction and an evaluation of their antimalarial activity. *Tetrahedron Lett.* **2014**, *55* (35), 4892−4894.
(87) Mekonnen, B.; Weiss, E.; Katz, E.; Ma, J. Y.; Ziffer, H.; Kyle, D. E. Synthesis and antimalarial activities of base-catalyzed adducts of 11-azaartemisinin. *Bioorg. Med. Chem.* **2000**, *8* (5), 1111−1116.
(88) Koi, H.; Takahashi, N.; Fuchi, Y.; Umeno, T.; Muramatsu, Y.; Seimiya, H.; Karasawa, S.; Oguri, H. A fully synthetic 6-aza-artemisinin bearing an amphiphilic chain generates aggregates and exhibits anti-cancer activities. *Org. Biomol. Chem.* **2020**, *18* (28), 5339−5343.
(89) Harmse, R.; Wong, H. N.; Smit, F. J.; Muller, J.; Hemphill, A.; N'Da, D. D.; Haynes, R. K. Activities of 11-Azaartemisinin and N-Sulfonyl Derivatives against Neospora caninum and Comparative Cytotoxicities. *ChemMedChem* **2017**, *12* (24), 2094−2098.
(90) Jana, S.; Iram, S.; Thomas, J.; Liekens, S.; Dehaen, W. Synthesis and anticancer activity of novel aza-artemisinin derivatives. *Bioorg. Med. Chem.* **2017**, *25* (14), 3671−3676.
(91) Sakaue, S.; Tsubakino, T.; Nishiyama, Y.; Ishii, Y. Oxidation of Aromatic-Amines with Hydrogen-Peroxide Catalyzed by Cetylpyridinium Heteropolyoxometalates. *J. Org. Chem.* **1993**, *58* (14), 3633−3638.
(92) Defoin, A. Simple preparation of nitroso benzenes and nitro benzenes by oxidation of anilines with H2O2 catalysed with molybdenum salts. *Synthesis* **2004**, *5*, 706−710.
(93) Colladon, M.; Scarso, A.; Strukul, G. Mild catalytic oxidation of secondary and tertiary amines to nitrones and N-oxides with H2O2 mediated by Pt(II) catalysts. *Green Chem.* **2008**, *10* (7), 793−798.
(94) Bernier, D.; Wefelscheid, U. K.; Woodward, S. Properties, Preparation and Synthetic Uses of Amine N-Oxides. An Update. *Org. Prep. Proced. Int.* **2009**, *41* (3), 173−210.
(95) Cope, A. C.; Foster, T. T.; Towle, P. H. Thermal Decomposition of Amine Oxides to Olefins and Dialkylhydroxylamines. *J. Am. Chem. Soc.* **1949**, *71* (12), 3929−3934.
(96) Marui, K.; Nomoto, A.; Ueshima, M.; Ogawa, A. Eco-friendly copper sulfate-catalyzed oxidation of amines to imines by hydrogen peroxide in water. *Tetrahedron Lett.* **2015**, *56* (10), 1200−1202.
(97) Wu, X.-F.; Petrosyan, A.; Ghochikyan, T. V.; Saghyan, A. S.; Langer, P. Metal-free oxidation of benzyl amines to imines. *Tetrahedron Lett.* **2013**, *54* (24), 3158−3159.
(98) Hawkins, E. G. E. Reactions of organic peroxides. Part XIV. Amino-peroxides from carbonyl compounds, primary amines, and hydrogen peroxide or hydroperoxide. *J. Chem. Soc. C* **1969**, *20*, 2686−2691.
(99) Hawkins, E. G. E. Reactions of organic peroxides. Part XI. Amino-peroxides from cyclic ketones. *J. Chem. Soc. C* **1969**, *20*, 2671−2677.
(100) Hawkins, E. G. E. Reactions of organic peroxides. Part XVI. Amino-peroxides from autoxidation of imines. *J. Chem. Soc. C* **1971**, *0*, 160−166.
(101) McCullough, K. J.; Mori, M.; Tabuchi, T.; Yamakoshi, H.; Kusabayashi, S.; Nojima, M. [3 + 2] Cycloadditions of carbonyl oxides to imines: an alternative approach to the synthesis of 1,2,4-dioxazolidines. *J. Chem. Soc., Perkin Trans. 1* **1995**, No. 1, 41−48.
(102) Ushigoe, Y.; Satake, S.; Masuyama, A.; Nojima, M.; McCullough, K. J. Synthesis of 1,2,4-dioxazolidine derivatives by the ozonolysis of indenes in the presence of primary amines. *J. Chem. Soc., Perkin Trans. 1* **1997**, *13*, 1939−1942.
(103) Griesbaum, K.; Liu, X.; Henke, H. N-Methoxy-1,2,4-Dioxazolidines by Ozonolysis Reactions. *J. Org. Chem.* **1998**, *63* (4), 1086−1089.
(104) Lee, K.-R.; Eun Lee, S.; Sung Huh, T. Syntheses of O-Methylated-1,2,4-dioxazolidines by Ozonolyses of O-Methylated Dioximes. *Bull. Korean Chem. Soc.* **2000**, *21* (10), 1039−1040.
(105) Kazakova, O. B.; Kazakov, D. V.; Yamansarov, E. Y.; Medvedeva, N. I.; Tolstikov, G. A.; Suponitsky, K. Y.; Arkhipov, D. E. Synthesis of triterpenoid-based 1,2,4-trioxolanes and 1,2,4-dioxazolidines by ozonolysis of allobetulin derivatives. *Tetrahedron Lett.* **2011**, *52* (9), 976−979.
(106) Schaap, A. P.; Prasad, G.; Siddiqui, S. Formation of 1,2,4-Dioxazolidines by Electron-Transfer Photooxygenation of Aziridines. *Tetrahedron Lett.* **1984**, *25* (29), 3035−3038.
(107) Schaap, A. P.; Prasad, G.; Gagnon, S. D. Formation of a 1,2,4-Dioxazolidine by Electron-Transfer Photo-Oxygenation of 1-Butyl-2,3-Diphenylaziridine. *Tetrahedron Lett.* **1983**, *24* (30), 3047−3050.
(108) Ishii, K.; Sone, T.; Shigeyama, T.; Noji, M.; Sugiyama, S. Photoreactions of beta-aziridinylacrylonitriles and acrylates with alkenes: the substituent effects on the formation of [3 + 2] cycloadducts. *Tetrahedron* **2006**, *62* (47), 10865−10878.
(109) Makhmudiyarova, N. N.; Khatmullina, G. M.; Rakhimov, R. S.; Meshcheryakova, E. S.; Ibragimov, A. G.; Dzhemilev, U. M. The First Example of Catalytic Synthesis of N-Aryl-Substituted Tetraoxazaspiroalkanes. *Tetrahedron* **2016**, *72*, 3277−3281.
(110) Makhmudiyarova, N. N.; Ishmukhametova, I. R.; Dzhemileva, L. U.; Tyumkina, T. V.; D'yakonov, V. A.; Ibragimov, A. G.; Dzhemilev, U. M. Synthesis and anticancer activity novel dimeric azatriperoxides. *RSC Adv.* **2019**, *9* (33), 18923−18929.
(111) Hawkins, E. G. E. *α*-Peroxyamines. *Angew. Chem., Int. Ed. Engl.* **1973**, *12* (10), 783−793.
(112) Fritz, H.; Kristinsson, H.; Mollenkopf, M.; Winkler, T. N-15 and C-13 Nmr-Study of Acylated Hydrazines - the Instability of

https://doi.org/10.1021/jacs.1c02249
J. Am. Chem. Soc. 2021, 143, 6634−6648

Trifluoroacethydrazide in the Solid-State. *Magn. Reson. Chem.* **1990**, *28* (4), 331−336.
(113) Kirby, A. J. *The Anomeric Effect and Related Stereoelectronic Effects at Oxygen*; Springer: Berlin, Heidelberg, 1983; p 149.
(114) Thatcher, G. R. J., Anomeric and Associated Stereoelectronic Effects. In *The Anomeric Effect and Associated Stereoelectronic Effects*; American Chemical Society: 1993; Vol. *539*, pp 6−25.
(115) Juaristi, E.; Cuevas, G. Recent Studies of the Anomeric Effect. *Tetrahedron* **1992**, *48* (24), 5019−5087.
(116) Juaristi, E.; Gomes, G. D.; Terent'ev, A. O.; Notario, R.; Alabugin, I. V. Stereoelectronic Interactions as a Probe for the Existence of the Intramolecular alpha-Effect. *J. Am. Chem. Soc.* **2017**, *139* (31), 10799−10813.
(117) Schenck, G. O.; Neumüller, O.-A.; Eisfeld, W. Zur photosensibilisierten Autoxydation der Steroide: Δ5-Steroid-7α-hydroperoxyde und −7-ketone durch Allylumlagerung von Δ6-Steroid-5α-hydroperoxyden. *Justus Liebigs Ann. Chem.* **1958**, *618* (1), 202−210.
(118) Yaremenko, I. A.; Vil', V. A.; Demchuk, D. V.; Terent'ev, A. O. Rearrangements of organic peroxides and related processes. *Beilstein J. Org. Chem.* **2016**, *12*, 1647−1748.
(119) Teng, J. I.; Kulig, M. J.; Smith, L. L.; Kan, G.; Van Lier, J. E. Sterol metabolism. XX. Cholesterol 7.beta.-hydroperoxide. *J. Org. Chem.* **1973**, *38* (1), 119−123.
(120) Yaremenko, I. A.; Terent'ev, A. O.; Vil', V. A.; Novikov, R. A.; Chernyshev, V. V.; Tafeenko, V. A.; Levitsky, D. O.; Fleury, F.; Nikishin, G. I. Approach for the Preparation of Various Classes of Peroxides Based on the Reaction of Triketones with H2O2: First Examples of Ozonide Rearrangements. *Chem. - Eur. J.* **2014**, *20* (32), 10160−10169.
(121) Harris, T.; Alabugin, I. V. Strain and stereoelectronics in cycloalkyne click chemistry. *Mendeleev Commun.* **2019**, *29* (3), 237−248.
(122) Harris, T.; Gomes, G. D.; Ayad, S.; Clark, R. J.; Lobodin, V. V.; Tuscan, M.; Hanson, K.; Alabugin, I. V. Twisted Cycloalkynes and Remote Activation of "Click" Reactivity. *Chem.* **2017**, *3* (4), 629−640.
(123) Frisch, M. J.; Trucks, G. W.; Schlegel, H. B.; Scuseria, G. E.; Robb, M. A.; Cheeseman, J. R.; Scalmani, G.; Barone, V.; Petersson, G. A.; Nakatsuji, H.; Li, X.; Caricato, M.; Marenich, A. V.; Bloino, J.; Janesko, B. G.; Gomperts, R.; Mennucci, B.; Hratchian, H. P.; Ortiz, J. V.; Izmaylov, A. F.; Sonnenberg, J. L.; Williams; Ding, F.; Lipparini, F.; Egidi, F.; Goings, J.; Peng, B.; Petrone, A.; Henderson, T.; Ranasinghe, D.; Zakrzewski, V. G.; Gao, J.; Rega, N.; Zheng, G.; Liang, W.; Hada, M.; Ehara, M.; Toyota, K.; Fukuda, R.; Hasegawa, J.; Ishida, M.; Nakajima, T.; Honda, Y.; Kitao, O.; Nakai, H.; Vreven, T.; Throssell, K.; Montgomery, J. A., Jr.; Peralta, J. E.; Ogliaro, F.; Bearpark, M. J.; Heyd, J. J.; Brothers, E. N.; Kudin, K. N.; Staroverov, V. N.; Keith, T. A.; Kobayashi, R.; Normand, J.; Raghavachari, K.; Rendell, A. P.; Burant, J. C.; Iyengar, S. S.; Tomasi, J.; Cossi, M.; Millam, J. M.; Klene, M.; Adamo, C.; Cammi, R.; Ochterski, J. W.; Martin, R. L.; Morokuma, K.; Farkas, O.; Foresman, J. B.; Fox, D. J. *Gaussian 16* Rev. A.03; Wallingford, CT, 2016.
(124) Adamo, C.; Barone, V. Toward reliable density functional methods without adjustable parameters: The PBE0 model. *J. Chem. Phys.* **1999**, *110* (13), 6158−6170.
(125) Grimme, S.; Antony, J.; Ehrlich, S.; Krieg, H. A consistent and accurate ab initio parametrization of density functional dispersion correction (DFT-D) for the 94 elements H-Pu. *J. Chem. Phys.* **2010**, *132* (15), 154104.
(126) Krishnan, R.; Binkley, J. S.; Seeger, R.; Pople, J. A. Self-consistent molecular orbital methods. XX. A basis set for correlated wave functions. *J. Chem. Phys.* **1980**, *72* (1), 650−654.
(127) Clark, T.; Chandrasekhar, J.; Spitznagel, G. W.; Schleyer, P. V. R. Efficient diffuse function-augmented basis sets for anion calculations. III. The 3-21+G basis set for first-row elements, Li−F. *J. Comput. Chem.* **1983**, *4* (3), 294−301.
(128) McLean, A. D.; Chandler, G. S.; Rothenberg, S.; Young, R. H.; Schaefer, H. F. Contracted Gaussian basis sets for molecular calculations. I. Second row atoms, Z = 11−18. *J. Chem. Phys.* **1980**, *72* (10), 5639−5648.
(129) Spitznagel, G. W.; Clark, T.; von Ragué Schleyer, P.; Hehre, W. J. An evaluation of the performance of diffuse function-augmented basis sets for second row elements, Na-Cl. *J. Comput. Chem.* **1987**, *8*, 1109−1116.
(130) Marenich, A. V.; Cramer, C. J.; Truhlar, D. G. Universal Solvation Model Based on Solute Electron Density and on a Continuum Model of the Solvent Defined by the Bulk Dielectric Constant and Atomic Surface Tensions. *J. Phys. Chem. B* **2009**, *113* (18), 6378−6396.
(131) Mardirossian, N.; Head-Gordon, M. Thirty years of density functional theory in computational chemistry: an overview and extensive assessment of 200 density functionals. *Mol. Phys.* **2017**, *115* (19), 2315−2372.
(132) Medvedev, M. G.; Bushmarinov, I. S.; Sun, J. W.; Perdew, J. P.; Lyssenko, K. A. Density functional theory is straying from the path toward the exact functional. *Science* **2017**, *355* (6320), 49−52.
(133) Mezei, P. D.; Csonka, G. I.; Kallay, M. Electron Density Errors and Density-Driven Exchange-Correlation Energy Errors in Approximate Density Functional Calculations. *J. Chem. Theory Comput.* **2017**, *13* (10), 4753−4764.
(134) Marjewski, A. A.; Medvedev, M. G.; Gerasimov, I. S.; Panova, M. V.; Perdew, J. P.; Lyssenko, K. A.; Dmitrienko, A. O. Interplay between test sets and statistical procedures in ranking DFT methods: the case of electron density studies. *Mendeleev Commun.* **2018**, *28* (3), 225−235.
(135) Medvedev, M. G.; Panova, M. V.; Chilov, G. G.; Bushmarinov, I. S.; Novikov, F. N.; Stroganov, O. V.; Zeifman, A. A.; Svitanko, I. V. Exhaustive conformational search for transition states: the case of catechol O-methyltransferase active site. *Mendeleev Commun.* **2017**, *27* (3), 224−227.
(136) Glendening, E. D.; Landis, C. R.; Weinhold, F. Natural bond orbital methods. *Wiley Interdiscip. Rev.: Comput. Mol. Sci.* **2012**, *2* (1), 1−42.
(137) Zefirov, N. S. Stereochemical Studies 0.21. General Equation of Relationship between Products Ratio and Conformational Equilibrium. *Tetrahedron* **1977**, *33* (20), 2719−2722.
(138) Seeman, J. I. The Curtin-Hammett Principle and the Winstein-Holness Equation - New Definition and Recent Extensions to Classical Concepts. *J. Chem. Educ.* **1986**, *63* (1), 42−48.
(139) Dunning, T. H. Gaussian-Basis Sets for Use in Correlated Molecular Calculations 0.1. The Atoms Boron through Neon and Hydrogen. *J. Chem. Phys.* **1989**, *90* (2), 1007−1023.
(140) Wierzbicki, A.; Salter, E. A.; Cioffi, E. A.; Stevens, E. D. Density functional theory and X-ray investigations of P- and M-hexamethylene triperoxide diamine and its dialdehyde derivative. *J. Phys. Chem. A* **2001**, *105* (38), 8763−8768.
(141) Alabugin, I. V.; Bresch, S.; Gomes, G. D. Orbital hybridization: a key electronic factor in control of structure and reactivity. *J. Phys. Org. Chem.* **2015**, *28* (2), 147−162.
(142) Kapp, J.; Schade, C.; El-Nahasa, A. M.; von Ragué Schleyer, P. Heavy Element π Donation Is Not Less Effective. *Angew. Chem., Int. Ed. Engl.* **1996**, *35* (19), 2236−2238.
(143) Alabugin, I. V.; Manoharan, M.; Buck, M.; Clark, R. J. Substituted anilines: The tug-of-war between pyramidalization and resonance inside and outside of crystal cavities. *J. Mol. Struct.: THEOCHEM* **2007**, *813* (1−3), 21−27.
(144) Glover, S. A.; White, J. M.; Rosser, A. A.; Digianantonio, K. M. Structures of N,N-Dialkoxyamides: Pyramidal Anomeric Amides with Low Amidicity. *J. Org. Chem.* **2011**, *76* (23), 9757−9763.
(145) Goerigk, L.; Sharma, R. The INV24 test set: how well do quantum-chemical methods describe inversion and racemization barriers? *Can. J. Chem.* **2016**, *94* (12), 1133−1143.
(146) Yaremenko, I. A.; Radulov, P. S.; Medvedev, M. G.; Krivoshchapov, N. V.; Belyakova, Y. Y.; Korlyukov, A. A.; Ilovaisky, A. I.; Terent'ev, A. O.; Alabugin, I. V. How to Build Rigid Oxygen-Rich Tricyclic Heterocycles from Triketones and Hydrogen Peroxide:

https://doi.org/10.1021/jacs.1c02249
J. Am. Chem. Soc. 2021, 143, 6634−6648

Control of Dynamic Covalent Chemistry with Inverse alpha-Effect. *J. Am. Chem. Soc.* **2020**, *142* (34), 14588−14607.
(147) Vil', V. A.; Barsegyan, Y. A.; Kuhn, L.; Ekimova, M. V.; Semenov, E. A.; Korlyukov, A. A.; Terent'ev, A. O.; Alabugin, I. V. Synthesis of unstrained Criegee intermediates: inverse alpha-effect and other protective stereoelectronic forces can stop Baeyer-Villiger rearrangement of gamma-hydroperoxy-gamma-peroxylactones. *Chem. Sci.* **2020**, *11* (20), 5313−5322.
(148) Vil', V. A.; Barsegyan, Y. A.; Barsukov, D. V.; Korlyukov, A. A.; Alabugin, I. V.; Terent'ev, A. O. Peroxycarbenium Ions as the ″Gatekeepers″ in Reaction Design: Assistance from Inverse Alpha-Effect in Three-Component beta-Alkoxy-beta-peroxylactones Synthesis. *Chem. - Eur. J.* **2019**, *25* (63), 14460−14468.
(149) Vil', V. A.; Gomes, G. D.; Ekimova, M. V.; Lyssenko, K. A.; Syroeshkin, M. A.; Nikishin, G. I.; Alabugin, I. V.; Terent'ev, A. O. Five Roads That Converge at the Cyclic Peroxy-Criegee Intermediates: BF3-Catalyzed Synthesis of beta-Hydroperoxy-beta-peroxylactones. *J. Org. Chem.* **2018**, *83* (21), 13427−13445.
(150) Vil', V. A.; Gomes, G. D.; Bityukov, O. V.; Lyssenko, K. A.; Nikishin, G. I.; Alabugin, I. V.; Terent'ev, A. O. Interrupted Baeyer-Villiger Rearrangement: Building A Stereoelectronic Trap for the Criegee Intermediate. *Angew. Chem., Int. Ed.* **2018**, *57* (13), 3372−3376.
(151) Sadovnichy, V.; Tikhonravov, A.; Voevodin, V.; Opanasenko, V. "Lomonosov": supercomputing at Moscow State University. In *Contemporary High Performance Computing*; CRC Press: Boca Raton, USA, 2013; pp 283−307.

https://doi.org/10.1021/jacs.1c02249
J. Am. Chem. Soc. 2021, 143, 6634−6648